Since January 2020 Elsevier has created a COVID-19 resource centre with free information in English and Mandarin on the novel coronavirus COVID-19. The COVID-19 resource centre is hosted on Elsevier Connect, the company's public news and information website.

Partial Differential Equations in Applied Mathematics 6 (2022) 100455

Contents lists available at ScienceDirect

Partial Differential Equations in Applied Mathematics

journal homepage: www.elsevier.com/locate/padiff

Fractal–fractional age-structure study of omicron SARS-CoV-2 variant transmission dynamics

Emmanuel Addai [a,b,*], Lingling Zhang [b,*], Joshua Kiddy K. Asamoah [c], Ama Kyerewaa Preko [d], Yarhands Dissou Arthur [e]

[a] College of Biomedical Engineering, Taiyuan University of Technology, Shanxi Taiyuan 030024, China
[b] Department of Mathematics, Taiyuan University of Technology, Shanxi Taiyuan 030024, China
[c] Department of Mathematics, Kwame Nkrumah University of Science and Technology, Kumasi, Ghana
[d] College of Teacher Education, Zhejiang Normal University, Zhejiang Jinhua, 321004, China
[e] Department of Mathematics Education, Akenten Appiah-Menka University of Skills Training and Entrepreneurial Development, Kumasi, Ghana

ARTICLE INFO

Keywords:
Omicron SARS-CoV-2 variant
Caputo–Fabrizio
Fractal–fractional derivatives
Numerical scheme
Newton polynomial

ABSTRACT

This paper proposes a new fractal–fractional age-structure model for the omicron SARS-CoV-2 variant under the Caputo–Fabrizio fractional order derivative. Caputo–Fabrizio fractal–fractional order is particularly successful in modelling real-world phenomena due to its repeated memory effect and ability to capture the exponentially decreasing impact of disease transmission dynamics. We consider two age groups, the first of which has a population under 50 and the second of a population beyond 50. Our results show that at a population dynamics level, there is a high infection and recovery of omicron SARS-CoV-2 variant infection among the population under 50 (Group-1), while a high infection rate and low recovery of omicron SARS-CoV-2 variant infection among the population beyond 50 (Group-2) when the fractal–fractional order is varied.

1. Introduction

Coronavirus disease (COVID-19) is a recent contagious disease caused by the SARS-COV-2 virus. One of the most well-known signs of this ailment is the appearance of minor to severe breathing issues. In some cases, the patient recovers without therapy. This virus exhibits symptoms include fever, coughing, and taste loss.[1–3] The infected people occasionally exhibit less typical symptoms including a sore throat, headache, or rash, among others.[1] In this setting, the age-related transmissibility of COVID-19 has emerged as a public health issue. The most severe health issues affect adults over the age of 60, with fatal consequences for population above 80 year.[4] This is because of the high rate of underlying health problems in elderly population.[4] Isolation play a significant role for limiting the spread of this disease since the signs of this virus sometimes do not show up, which facilitate quick transmission. A rise in anxiety and despair has been documented in the general population, particularly among persons who have been isolated for lengthy periods of time, according to early study.[5,6] Recent research has shown that even when the infected individual has recovery from this disease, depressive symptoms are prevalent among many of the elderly population.[7,8] SAR-CoV-2, like any other viruses, develops throughout time. The numerous of alterations have little or no impact on the virus characteristics. However, some of these changes might affect the virus characteristics, such as how easily it transmit from one person to another, the degree and severity of the disease it causes, or the effectiveness of vaccines, therapeutic medications, and diagnostic tests. The Omicron (B.1.1.529/21K) variety was discovered in South Africa's Gauteng Province, before the end of November 2021. Based on PCR-confirmed cases, the estimated reproduction number as of November 18th, 2021, was 2.3, which was the highest recorded during any of the previous three waves.[9] The SARS-CoV-2 Omicron (B.1.1.529) VOC (variant of concern) has been found all over the world, drawing a lot of attention because early evidence suggests it spreads and reinfects more easily than the Delta variant.[9,10] Other VOC have been found to include mutations similar to those in omicron's spike, which have been demonstrated to improve transmissibility and confer varied degrees of escape from neutralizing antibodies.[10–14] Nevertheless, various Omicron mutations have not been observed on previous VOC, nor have the functional effects of these mutations been characterized in a stringent manner. Concerns have been raised due to the fact that the efficacy of vaccines and therapeutic antibodies may be effectively decrease when used against Omicron because many undiscovered Omicron mutations are located inside antibody epitopes. These worries have sparked decisions about policy and research priorities that will have broad effects.[10] When dealing with an epidemic, it is essential to accurately predict what will occur in the future, understand how to stop it from spreading, and provide the appropriate preventative measures before

* Corresponding authors.
E-mail addresses: papayawewit@gmail.com (E. Addai), tyutzll@126.com (L. Zhang), jkkasamoah@knust.edu.gh (J.K.K. Asamoah).

https://doi.org/10.1016/j.padiff.2022.100455
Received 11 July 2022; Received in revised form 7 October 2022; Accepted 11 October 2022

it is too late. Numerous researchers from various academic disciplines have contributed to the study of COVID-19 (Omicron variant), (see Refs. 15–25). As a result, many mathematical formulations relating to the prediction of COVID-19 have been developed see Refs. 26–31. Indeed, these models show the population dynamics of COVID-19 and how to control the disease using the ideas of integer order and optimal control studies. Despite the results obtained through integer-order equations and optimal control, the results obtained through fractional-order equations give other dynamical results since they depict the effects of memory on the dynamics of biological processes. In the study of fractional calculus in mathematical modelling, there are three most popular fractional derivatives: Caputo (C), Caputo–Fabrizio (CF), and Atangana–Baleanu–Caputo (ABC). For example the work in Ref. 32 studied the dynamical effects of these fractional derivatives on the dynamical analysis of Q fever. They indicated in their studies that Atangana–Baleanu fractional differential operator captures a greater number of susceptibilities while simultaneously accounting for a smaller number of infections than the other Caputo and Caputo–Fabrizio. The work of Ref. 33, Ref. 34 and Ref. 35 also gives some accounts on the use of fractional derivatives on COVID-19 and other diseases. The work in Ref. 36 presented chaos study of tumor and effector cells in fractional tumor-immune model for cancer treatment. Ref. 37 presented numerical investigations on COVID-19 model through singular and non-singular fractional operators, thus Caputo, Caputo–Fabrizio and Atangana–Baleanu. Ref. 38 gives s theoretical study of the Caputo–Fabrizio fractional modelling for hearing loss due to Mumps virus with optimal control. The work in Ref. 39 and Ref. 40 studied the wavelet dynamics using fractional analysis. Also, fractional derivatives' usefulness in the dynamism of SARS-CoV-2 and Ebola–Malaria spread in a population is presented in Ref. 41 and Ref. 42, respectively. The work in Ref. 43 studied a mathematical model of COVID-19 spread in Turkey and South Africa using fractional analysis. In 2017, Atangana Ref. 44 introduced the concept of fractal–fractional derivatives, thus connecting fractal and fractional calculus to predict complex systems. The idea is essential because numerous phenomena in our natural world take the form of repeated patterns and memory effects. This operator is a powerful mathematical tool for modelling complex real-world problems and supports single classical and nonlocal differential and integral operators. Mathematical epidemiological researchers have studied various diseases using fractal–fractional derivatives to analyse the complicated dynamics of infectious disease dissemination in an environment. In Ref. 45 presented a model and analysis of the dynamics of HIV/AIDS with non-singular fractional and fractal–fractional operators. The author in Ref. 46 applied fractal–fractional derivative to study the dynamics of Q fever. Some other application of fractal–fractional operator can be found in Refs. 47–52. The work in Ref. 53 studied an optimal control and cost-effectiveness analysis of a new COVID-19 model for Omicron strains. They estimated the basic reproduction number as 1.5188. Changjin[54] presented Lyapunov stability and wave analysis of the COVID-19 Omicron variant using actual data with fractional analysis. Simulations were made to understand the behaviour of the virus. The work in Ref. 55 studied the influence of NPIs and vaccination of the SARS-CoV-2 Omicron variant. They showed that the disease-induced death shows periodic oscillation. Cai[56] presented a data-derived prediction dynamics of the Omicron variant. Farman[57] introduced an Atangana–Baleanu fractal–fractional model for the COVID-19 Omicron variant and showed some mathematical analysis of their model. They proved the Omicron wave's bounded solution and presented some numerical simulations. Farman[57] did not group their model in the age category. This paper applies a fractal–fractional operator to formulate two age-structure models for the Omicron SARS-CoV-2 variant. The primary goals of this research are to determine the extent of the COVID-19 outbreak and the Omicron variant transmission, to predict potential future outcomes in two different age groups, and to assess the impact of the Omicron SARS-CoV-2 variant on the elderly in the community. Furthermore, to use the Caputo–Fabrizio derivative to capture the exponential decay of the virus in two separate age groups since there is no single mathematical formulation of a two-age-structure Omicron SARS-CoV-2 variant model using Caputo–Fabrizio fractal–fractional dynamics to capture the repeated patterns and memory of the exponential decay of the Omicron variant.

The structure of the paper is as follows: In Section 2, we briefly discuss the essential definitions and their relationship to fractal–fractional operators. In Section 3, we formulate the proposed model in classical and fractional cases. In Section 4, we discusses and examines the existence-uniqueness using fixed point theorem. In Section 5, we discuss the Hyers–Ulam stability regarding our proposed model. The numerical answers to the omicron SARS-CoV-2 variant transmission are found in Section 6, thus using the Caputo–Fabrizio technique and Newton polynomial approximation. Mathematical simulations are performed in Section 7 using Matlab, and the results are discussed briefly in Section 8 before the conclusion of our study.

2. Preliminaries

In this section, we recall the Caputo–Fabrizio definitions related to fractional calculus and some lemma.

Definition 2.1 (*Refs. 44–46*)**.** The fractal–fractional (FF) derivative g in the Riemann–Liouville (RL) case with exponential kernel known as Caputo fractal–fractional derivative is given as

$$^{CFF}D_{0,t}^{\mu_*,\nu_*}[g(t)] = \frac{M^*(\mu_*)}{1-\mu_*}\frac{d}{dt^{\nu_*}}\int_0^t \exp\left(\frac{-\mu_*}{1-\mu_*}(t-x)\right) g(x)dx,$$

with $n-1 < \mu_*, \nu_* \leq n \in \mathbb{N}$, and $M^*(0) = M(1) = 1$.

Definition 2.2 (*Refs. 44, 46*)**.** The fractal–fractional integral of the above fractional derivative is given as

$$^{CFF}I_{0,t}^{\mu_*,\nu_*}[g(t)] = \frac{\mu_*\nu_*}{M^*(\mu_*)}\int_0^t x^{*\mu_*-1}g(x^*)dx^* + \frac{\nu_*(1-\mu_*)t^{\nu_*-1}g(t)}{M^*(\mu_*)}.$$

Lemma 2.3 (*Ref. 58*)**.** *If we suppose that Krasnoselskii's fixed point theorem $\boldsymbol{E} \subset \boldsymbol{K}$, be an empty closed convex subset of $\boldsymbol{K}^*$ and there exist two operator $\mathbf{A}_y$ and $\mathbf{A}_x$, thus*

(i) $\mathbf{A}_x\mathbf{X} + \mathbf{A}_y\mathbf{Y} \in \boldsymbol{E}$, $\forall \mathbf{Y} \in \boldsymbol{E}$

(ii) $\mathbf{A}_x$ *is contraction and* $\mathbf{A}_y$ *continuous and compact. Then,* $\exists$ *at least one solution* $\mathbf{Y} \in \boldsymbol{E}$ *such that*

$$\mathbf{A}_x Y + \mathbf{A}_y Y = \mathbf{Y}.$$

Lemma 2.4 (*Ref. 41*)**.** *Suppose that $Y(0) \in C([0,\eta])$, then the solution of fractal–fractional differential equation*

$$\begin{cases} {}^{CFF}D_t^{\mu_*\nu_*}Y(t) = \Phi(t, Y(t)), \\ Y(0) = Y_0, \end{cases}$$

is given as

$$Y(t) = Y(0) + \frac{\nu_*(1-\mu_*)t^{\nu_*-1}}{G(\mu_*)}\Phi(t,Y(t)) + \frac{\mu_*\nu_*}{G(\mu_*)}\int_0^t \tau^{\nu_*-1}\Phi(\tau,Y(\tau))d\tau.$$

3. Model formulation

We consider the entire population into two age groups, where we represent the Group-1 by people below 50 years old, thus young population (<50 years old), and the Group-2 includes the people from 50 years, thus aged population (≥50 years old). We consider the compartments as susceptible (S), exposed (E), COVID-infected without Omicron (I), omicron-infected (O), quarantine (K), recovered (R). Each population ($SEIOKR$) consist of $S_1 + E_1 + O_1 + I_1 + K_1 + R_1$ for Group-1 population and $S_2 + E_2 + I_2 + O_2 + K_2 + R_2$ for Group-2 population. $N(t) = N_1 + N_2$ and $N_i = S_i + E_i + I_i + O_i + K_i + R_i$ where $i = 1, 2$. Table 1 provides a detailed description of the proposed model

parameters. As a result, the set of differential equations below describes the two age-structure model for the omicron SARS-CoV-2 variant.

$$
\begin{cases}
\frac{dS_1(t)}{dt} = \Lambda_1 - (\mu_1+\gamma_1)S_1 + \delta_1 R_1 \\
\quad -S_1\left(\beta_1 E_1 - \beta_2 E_2 - \beta_3 I_1 - \beta_4 I_2 - \beta_5 O_1 - \beta_6 O_2 - \Lambda_2\right), \\
\frac{dE_1(t)}{dt} = \beta_1(1-\epsilon_1-\epsilon_2)S_1E_1 + \beta_2(1-\epsilon_1-\epsilon_2)S_1E_2 \\
\quad -(\mu_1+\alpha_1+\theta_1+\sigma_1)E_1 - \Lambda_2 E_1, \\
\frac{dI_1(t)}{dt} = \beta_3 S_1 I_1 + \beta_4 S_1 I_2 + \alpha_1 E_1 - (\mu_1+\kappa_1+\eta_1+\rho_1)I_1 - \Lambda_2 I_1, \\
\frac{dO_1(t)}{dt} = \beta_1\epsilon_2 S_1 E_1 + \beta_2\epsilon_2 S_1 E_2 + \beta_5 S_1 O_1 + \beta_6 S_1 O_2 + \sigma_1 E_1 \\
\quad -(\omega_1+\vartheta_1+\nu_1+\mu_1)O_1 - \Lambda_2 O_1, \\
\frac{dK_1(t)}{dt} = \gamma_1 S_1 + \theta_1 E_1 + \eta_1 I_1 + \omega_1 O_1 - \mu_1 K_1 - \Lambda_2 K_1, \\
\frac{dR_1(t)}{dt} = \rho_1 I_1 + \vartheta_1 O_1 - (\delta_1+\mu_1)R_1 - \Lambda_2 R_1, \\
\frac{dS_2(t)}{dt} = \Lambda_2 S_1 - (\mu_2+\gamma_2)S_2 + \delta_2 R_2 \\
\quad -S_2\left(\beta_7 E_1 - \beta_8 E_2 - \beta_9 I_1 - \beta_{10} I_2 - \beta_{11} O_1 - \beta_{12} O_2\right), \\
\frac{dE_2(t)}{dt} = \Lambda_2 E_1 + \beta_7(1-\epsilon_3-\epsilon_4)S_2E_1 + \beta_8(1-\epsilon_3-\epsilon_4)S_2E_2 \\
\quad -(\mu_2+\alpha_2+\theta_2+\sigma_2)E_2, \\
\frac{dI_2(t)}{dt} = \Lambda_2 I_1 + \beta_9 S_2 I_1 + \beta_{10} S_2 I_2 + \alpha_2 E_2 - (\mu_2+\kappa_2+\eta_2+\rho_2)I_2, \\
\frac{dO_2(t)}{dt} = \Lambda_2 O_1 + \beta_7\epsilon_4 S_2 E_1 + \beta_8\epsilon_4 S_2 E_2 + \beta_{11} S_2 O_1 \\
\quad +\beta_{12} S_2 O_2 + \sigma_2 E_2 - (\omega_2+\vartheta_2+\nu_2+\mu_2)O_2, \\
\frac{dK_1(t)}{dt} = \Lambda_2 K_1 + \gamma_2 S_2 + \theta_2 E_2 + \eta_2 I_2 + \omega_2 O_2 - \mu_2 K_2, \\
\frac{dR_2(t)}{dt} = \Lambda_2 R_1 + \rho_2 I_2 + \vartheta_2 O_2 - (\delta_2+\mu_2)R_2.
\end{cases}
\tag{3.1}
$$

And our considered CF fractal–fractional two-age structure model for Omicron SARS-CoV-2 variant is defined as follows;

$$
\begin{cases}
{}^{CFF}D_t^{\mu_*,\nu_*} S_1(t) = \Lambda_1 - (\mu_1+\gamma_1)S_1 + \delta_1 R_1 \\
\quad -S_1\left(\beta_1 E_1 - \beta_2 E_2 - \beta_3 I_1 - \beta_4 I_2 - \beta_5 O_1 - \beta_6 O_2 - \Lambda_2\right), \\
{}^{CFF}D_t^{\mu_*,\nu_*} E_1(t) = \beta_1(1-\epsilon_1-\epsilon_2)S_1E_1 + \beta_2(1-\epsilon_1-\epsilon_2)S_1E_2 \\
\quad -(\mu_1+\alpha_1+\theta_1+\sigma_1)E_1 - \Lambda_2 E_1, \\
{}^{CFF}D_t^{\mu_*,\nu_*} I_1(t) = \beta_3 S_1 I_1 + \beta_4 S_1 I_2 + \alpha_1 E_1 \\
\quad -(\mu_1+\kappa_1+\eta_1+\rho_1)I_1 - \Lambda_2 I_1, \\
{}^{CFF}D_t^{\mu_*,\nu_*} O_1(t) = \beta_1\epsilon_2 S_1 E_1 + \beta_2\epsilon_2 S_1 E_2 + \beta_5 S_1 O_1 \\
\quad +\beta_6 S_1 O_2 + \sigma_1 E_1 - (\omega_1+\vartheta_1+\nu_1+\mu_1)O_1 - \Lambda_2 O_1, \\
{}^{CFF}D_t^{\mu_*,\nu_*} K_1(t) = \gamma_1 S_1 + \theta_1 E_1 + \eta_1 I_1 + \omega_1 O_1 - \mu_1 K_1 - \Lambda_2 K_1, \\
{}^{CFF}D_t^{\mu_*,\nu_*} R_1(t) = \rho_1 I_1 + \vartheta_1 O_1 - (\delta_1+\mu_1)R_1 - \Lambda_2 R_1, \\
{}^{CFF}D_t^{\mu_*,\nu_*} S_2(t) = \Lambda_2 S_1 - (\mu_2+\gamma_2)S_2 + \delta_2 R_2 \\
\quad -S_2\left(\beta_7 E_1 - \beta_8 E_2 - \beta_9 I_1 - \beta_{10} I_2 - \beta_{11} O_1 - \beta_{12} O_2\right), \\
{}^{CFF}D_t^{\mu_*,\nu_*} E_2(t) = \Lambda_2 E_1 + \beta_7(1-\epsilon_3-\epsilon_4)S_2E_1 \\
\quad +\beta_8(1-\epsilon_3-\epsilon_4)S_2E_2 - (\mu_2+\alpha_2+\theta_2+\sigma_2)E_2, \\
{}^{CFF}D_t^{\mu_*,\nu_*} I_2(t) = \Lambda_2 I_1 + \beta_9 S_2 I_1 + \beta_{10} S_2 I_2 \\
\quad +\alpha_2 E_2 - (\mu_2+\kappa_2+\eta_2+\rho_2)I_2, \\
{}^{CFF}D_t^{\mu_*,\nu_*} O_2(t) = \Lambda_2 O_1 + \beta_7\epsilon_4 S_2 E_1 + \beta_8\epsilon_4 S_2 E_2 \\
\quad +\beta_{11} S_2 O_1 + \beta_{12} S_2 O_2 + \sigma_2 E_2 - (\omega_2+\vartheta_2+\nu_2+\mu_2)O_2, \\
{}^{CFF}D_t^{\mu_*,\nu_*} R_2(t) = \Lambda_2 K_1 + \gamma_2 S_2 + \theta_2 E_2 + \eta_2 I_2 + \omega_2 O_2 - \mu_2 K_2, \\
{}^{CFF}D_t^{\mu_*,\nu_*} R_2(t) = \Lambda_2 R_1 + \rho_2 I_2 + \vartheta_2 O_2 - (\delta_2+\mu_2)R_2.
\end{cases}
\tag{3.2}
$$

4. Existence and uniqueness results

In this section, we examine the existence and uniqueness of our epidemiological model. It is important to establish whether or not such a dynamical problem actually exists in any epidemic model. The solution to this evaluation is guaranteed by the fixed point theory. We try to apply the same approach to the above model from the viewpoint of Banach and Krasnoselskii's fixed point theory (3.2) to study existence and uniqueness results. Regarding to the aforementioned requirement, we rewrite the right-hand side of the model (3.2) as follows;

$$
\begin{cases}
{}^{CFF}D_t^{\mu_*,\nu_*} S_1(t) = Y_1(t,S_i,E_i,I_i,O_i,K_i,R_i), \\
{}^{CFF}D_t^{\mu_*,\nu_*} E_1(t) = Y_2(t,S_i,E_i,I_i,O_i,K_i,R_i), \\
{}^{CFF}D_t^{\mu_*,\nu_*} I_1(t) = Y_3(t,S_i,E_i,I_i,O_i,K_i,R_i), \\
{}^{CFF}D_t^{\mu_*,\nu_*} O_1(t) = Y_4(t,S_i,E_i,I_i,O_i,K_i,R_i), \\
{}^{CFF}D_t^{\mu_*,\nu_*} K_1(t) = Y_5(t,S_i,E_i,I_i,O_i,K_i,R_i), \\
{}^{CFF}D_t^{\mu_*,\nu_*} R_1(t) = Y_6(t,S_i,E_i,I_i,O_i,K_i,R_i), \\
{}^{CFF}D_t^{\mu_*,\nu_*} S_2(t) = Y_7(t,S_i,E_i,I_i,O_i,K_i,R_i), \\
{}^{CFF}D_t^{\mu_*,\nu_*} E_2(t) = Y_8(t,S_i,E_i,I_i,O_i,K_i,R_i), \\
{}^{CFF}D_t^{\mu_*,\nu_*} I_2(t) = Y_9(t,S_i,E_i,I_i,O_i,K_i,R_i), \\
{}^{CFF}D_t^{\mu_*,\nu_*} O_2(t) = Y_{10}(t,S_i,E_i,I_i,O_i,K_i,R_i), \\
{}^{CFF}D_t^{\mu_*,\nu_*} K_2(t) = Y_{11}(t,S_i,E_i,I_i,O_i,K_i,R_i), \\
{}^{CFF}D_t^{\mu_*,\nu_*} R_2(t) = Y_{12}(t,S_i,E_i,I_i,O_i,K_i,R_i),
\end{cases}
\tag{4.1}
$$

for all $i = 1, 2$, where

$$
\begin{cases}
Y_1(t,S_i,E_i,I_i,O_i,K_i,R_i) = \Lambda_1 - (\mu_1+\gamma_1)S_1 + \delta_1 R_1 \\
\qquad - S_1\left(\beta_1 E_1 - \beta_2 E_2 - \beta_3 I_1 - \beta_4 I_2 - \beta_5 O_1 - \beta_6 O_2 - \Lambda_2\right), \\
Y_2(t,S_i,E_i,I_i,O_i,K_i,R_i) = \beta_1(1-\epsilon_1-\epsilon_2)S_1E_1 + \beta_2(1-\epsilon_1-\epsilon_2)S_1E_2 \\
\qquad - (\mu_1+\alpha_1+\theta_1+\sigma_1)E_1 - \Lambda_2 E_1, \\
Y_3(t,S_i,E_i,I_i,O_i,K_i,R_i) = \beta_3 S_1 I_1 + \beta_4 S_1 I_2 + \alpha_1 E_1 - (\mu_1+\kappa_1+\eta_1+\rho_1)I_1 - \Lambda_2 I_1, \\
Y_4(t,S_i,E_i,I_i,O_i,K_i,R_i) = \beta_1\epsilon_2 S_1 E_1 + \beta_2\epsilon_2 S_1 E_2 + \beta_5 S_1 O_1 + \beta_6 S_1 O_2 + \sigma_1 E_1 \\
\qquad - (\omega_1+\vartheta_1+\nu_1+\mu_1)O_1 - \Lambda_2 O_1, \\
Y_5(t,S_i,E_i,I_i,O_i,K_i,R_i) = \gamma_1 S_1 + \theta_1 E_1 + \eta_1 I_1 + \omega_1 O_1 - \mu_1 K_1 - \Lambda_2 K_1, \\
Y_6(t,S_i,E_i,I_i,O_i,K_i,R_i) = \rho_1 I_1 + \vartheta_1 O_1 - (\delta_1+\mu_1)R_1 - \Lambda_2 R_1, \\
Y_7(t,S_i,E_i,I_i,O_i,K_i,R_i) = \Lambda_2 S_1 - (\mu_2+\gamma_2)S_2 + \delta_2 R_2 \\
\qquad - S_2\left(\beta_7 E_1 - \beta_8 E_2 - \beta_9 I_1 - \beta_{10} I_2 - \beta_{11} O_1 - \beta_{12} O_2\right), \\
Y_8(t,S_i,E_i,I_i,O_i,K_i,R_i) = \Lambda_2 E_1 + \beta_7(1-\epsilon_3-\epsilon_4)S_2E_1 + \beta_8(1-\epsilon_3-\epsilon_4)S_2E_2 \\
\qquad - (\mu_2+\alpha_2+\theta_2+\sigma_2)E_2, \\
Y_9(t,S_i,E_i,I_i,O_i,K_i,R_i) = \Lambda_2 I_1 + \beta_9 S_2 I_1 + \beta_{10} S_2 I_2 + \alpha_2 E_2 \\
\qquad - (\mu_2+\kappa_2+\eta_2+\rho_2)I_2, \\
Y_{10}(t,S_i,E_i,I_i,O_i,K_i,R_i) = \Lambda_2 O_1 + \beta_7\epsilon_4 S_2 E_1 + \beta_8\epsilon_4 S_2 E_2 \\
\qquad + \beta_{11} S_2 O_1 + \beta_{12} S_2 O_2 + \sigma_2 E_2 \\
\qquad - (\omega_2+\vartheta_2+\nu_2+\mu_2)O_2, \\
Y_{11}(t,S_i,E_i,I_i,O_i,K_i,R_i) = \Lambda_2 K_1 + \gamma_2 S_2 + \theta_2 E_2 + \eta_2 I_2 + \omega_2 O_2 - \mu_2 K_2, \\
Y_{12}(t,S_i,E_i,I_i,O_i,K_i,R_i) = \Lambda_2 R_1 + \rho_2 I_2 + \vartheta_2 O_2 - (\delta_2+\mu_2)R_2.
\end{cases}
\tag{4.2}
$$

Assume that $C^1([0,T],R^+)$ be the Banach space endowed with supremum norm

$$\|Y\| = \|Y_1(S_i,E_i,I_i,O_i,K_i,R_i)\| = \sup_{t\in[0,T]} |Y(t)|,$$

where $|Y(t)| = |S_i|+|E_i|+|I_i|+|O_i|+|K_i|+|R_i|$ and $S_i, E_i, I_i, O_i, K_i, R_i \in C^1([0,T],R^+)$, and for all $i = 1, 2$.

Table 1
Parameter definitions.

Parameter	Definition
Λ_1	Recruitment rate of Group 1
Λ_2	Recruitment rate of Group 2
β_1, β_2	Effective contact rate between S_1/E_1 and S_1/E_2
β_3, β_4	Effective contact rate between S_1/I_1 and S_1/I_2
β_5, β_6	Effective contact rate between S_1/O_1 and S_1/O_2
β_7, β_8	Effective contact rate between S_2/E_1 and S_2/E_2
β_9, β_{10}	Effective contact rate between S_2/I_1 and S_2/I_2
β_{11}, β_{12}	Effective contact rate between S_2/O_1 and S_2/O_2
μ_1, μ_2	Natural death rate for Group 1 and Group 2
γ_1, γ_2	The rate of S_1 and S_2 who have been in quarantine
δ_1, δ_2	The rate of recovering from R_1 and R_2
ϵ_1, ϵ_2	The rate of recognizing non-omicron variant and omicron variant in group 1
ϵ_3, ϵ_4	The rate of recognizing non-omicron variant and omicron variant in group 2
(α_1, α_2)	The screening rate for the individuals infected with COVID-19 in both group 1 and group 2
θ_1, θ_2	The rate of quarantine people infected without symptoms in both group 1 and group 2
σ_1, σ_2	The rate of effective screening for the individuals infected with omicron variant in group 1 and group 2
κ_1, κ_2	disease induce rate in group 1 and group 2
ρ_1, ρ_2	The rate of people recovery from infection in both group 1 and group 2
η_1, η_2	The percentage of people in quarantine who are infected with COVID-19 in both group 1 and group 2
ϑ_1, ϑ_2	The rate of people recovery from omicron variant in both group 1 and group 2
ν_1, ν_2	Disease induce rate in group 1 and group 2
ω_1, ω_2	The percentage of people in quarantine who are infected with omicron variant in both group 1 and group 2

From (3.2), the developed model (4.1) can be written in the form of the following

$$\begin{cases} {}^{CFF}D_t^{\mu_*,\nu_*}Y(t) = \nu_* t^{\nu_*-1}\Phi(t, Y(t)), \ t \in [0, T], \\ Y(0) = Y_0, \end{cases} \tag{4.3}$$

where

$$Y(t) = \begin{cases} S_i(t), \\ E_i(t), \\ I_i(t), \\ O_i(t), \\ K_i(t), \\ R_i(t), \end{cases} \quad Y_0 = \begin{cases} S_i(0), \\ E_i(0), \\ I_i(0), \\ O_i(0), \\ K_i(0), \\ R_i(0), \end{cases} \quad \Phi(t, Y(t)) = \begin{cases} Y_1(t, S_i, E_i, I_i, O_i, R_i), \\ Y_2(t, S_i, E_i, I_i, O_i, R_i), \\ Y_3(t, S_i, E_i, I_i, O_i, R_i), \\ Y_4(t, S_i, E_i, I_i, O_i, R_i), \\ Y_5(t, S_i, E_i, I_i, O_i, R_i) \\ Y_6(t, S_i, E_i, I_i, O_i, R_i) \\ Y_7(t, S_i, E_i, I_i, O_i, R_i), \\ Y_8(t, S_i, E_i, I_i, O_i, R_i), \\ Y_9(t, S_i, E_i, I_i, O_i, R_i), \\ Y_{10}(t, S_i, E_i, I_i, O_i, R_i), \\ Y_{11}(t, S_i, E_i, I_i, O_i, R_i) \\ Y_{12}(t, S_i, E_i, I_i, O_i, R_i). \end{cases} \tag{4.4}$$

In view of Definition 2.5, the fractal–fractional problem (4.3) is equivalent to the following fractal–fractional integral equation

$$\begin{aligned} {}^{CFF}I_t^{\mu_*\nu_*}[Y(t)] = Y_0 &+ \frac{\nu_*(1-\mu_*)t^{\nu_*-1}}{G(\mu_*)}Y(t) \\ &+ \frac{\mu_*\nu_*}{G(\mu_*)}\int_0^t \tau^{\nu_*-1}\Phi(\tau, Y(\tau))d\tau. \end{aligned} \tag{4.5}$$

From here, we let $Z_* = C([0, T])$ be the Banach space, assuming that the following hypotheses hold

(H_1) There will be a positive constants $\mathbf{W}, \mathbf{M}$, and $\mathbf{k} \in [0, 1)$ such that

$$\Phi(t, Y(t)) \le \mathbf{W}|Y|^{\mathbf{k}} + \mathbf{M}.$$

(H_2) There exist a positive constant $\mathbf{C}_p > 0$ for all $Y, \tilde{Y} \in Z_*$ then

$$|\Phi(t, Y(t)) - \Phi(t, \tilde{Y}(t))| \le \mathbf{C}_*[|Y - \tilde{Y}|].$$

Also, we define operator $\mathbf{A}_p : Z_* \to Z_*$ such that

$$\mathbf{A}_pY(t) = \Omega_1^*Y(t) + \Omega_2^*Y(t),$$

basically, we can see that

$$\begin{cases} \Omega_1^*Y(\sigma) = Y_0 + \frac{\nu_*(1-\mu_*)t^{\nu_*-1}}{G(\mu_*)}Y(t), \\ \Omega_2^*Y(\sigma) = \frac{\mu_*\nu_*}{G(\mu_*)}\int_0^t \tau^{\nu_*-1}\Phi(\tau, Y(\tau))d\tau. \end{cases} \tag{4.6}$$

From this knowledge (4.5) then can be written as

$$\begin{cases} \mathbf{A}_pY(\sigma) = Y_0 + \frac{\nu_*(1-\mu_*)t^{\nu_*-1}}{G(\mu_*)}Y(t) + \frac{\mu_*\nu_*}{G(\mu_*)}\int_0^t \tau^{\nu_*-1}\Phi(\tau, Y(\tau))d\tau. \end{cases} \tag{4.7}$$

Theorem 4.1. *Suppose that (H_1) and (H_2) hold, such that, $\frac{\nu_*(1-\mu_*)t^{\nu_*-1}}{G(\mu_*)}\mathbf{C}_* < 1$, then the two-age structure model for omicron SARS-CoV-2 variant has at least one solution.*

Proof. We split the proof into two parts for ease of understanding.

Step 1. We show that Ω_1^* is contraction. If so, let $\tilde{Y} \in \Pi$, where $\Pi = \{Y \in \mathbf{Z}_* : \ \|Y\| \le \varphi, \ \varphi > 0\}$ is a close convex set, thus

$$\begin{aligned} |\Omega_1^*Y(t) - \Omega_2^*Y(t)| &= \frac{\nu_*(1-\mu_*)t^{\nu_*-1}}{G(\mu_*)}\max_{t\in[0,T]}|\Phi(t, Y(t)) - \Phi(t, \tilde{Y}(t))|, \\ &\le \frac{\nu_*(1-\mu_*)t^{\nu_*-1}}{G(\mu_*)}\mathbf{C}_*\|Y - \tilde{Y}\|. \end{aligned} \tag{4.8}$$

Thus,

$$\|\Omega_1^*Y(t) - \Omega_2^*Y(t)\| \le \frac{\nu_*(1-\mu_*)t^{\nu_*-1}}{G(\mu_*)}\mathbf{C}_*\|Y - \tilde{Y}\|.$$

Hence Ω_1^* is contraction since $\frac{\nu_*(1-\mu_*)t^{\nu_*-1}}{G(\mu_*)}\mathbf{C}_* < 1$.

Step 2. We show that Ω_2^* is completely continuous, for all $Y \in \Pi$, then Ω_2^* will be continuous as Y is continuous, thus

$$\begin{aligned} \|\Omega_2^*(Y)\| &= \max_{t\in[0,T]}|\frac{\mu_*\nu_*}{G(\mu_*)}\int_0^t \tau^{\nu_*-1}\Phi(\tau, Y(\tau))d\tau|, \\ &\le \frac{\mu_*\nu_*}{G(\mu_*)}\int_0^t |\tau^{\nu_*-1}|\ |\Phi(\tau, Y(\tau))|d\tau. \\ &\le \frac{\mu_*}{G(\mu_*)}[W_*|Y|^{k_*} + M_*]. \end{aligned} \tag{4.9}$$

Hence Ω_2^* is boundedness. For equicontinuous, let $t_1, \ t_2 \in [0, T]$, such that

$$\begin{aligned} |(\Omega_2^*Y)(\sigma_1) - (\Omega_2^*Y)(\sigma_2)| &= \frac{\mu_*\nu_*}{G(\mu_*)}\Big|\int_0^t t_1^{\nu_*-1}\Phi(\tau, Y(\tau))d\tau \\ &\quad - \int_0^t t_2^{\nu_*-1}\Phi(\tau, Y(\tau))d\tau\Big| \\ &\le \frac{\mu_*[W_*|Y|^{k_*} + M_*]}{G(\mu_*)}[t_1 - t_2]. \end{aligned} \tag{4.10}$$

As $\sigma_1 \to \sigma_2$, then $|(\Omega_2^*Y)(t_1) - (\Omega_2^*Y)(t_2)| \to 0$. In view of the well known Arzela–Ascoli theorem operator Ω_2^* is equicontinuous and compact. Therefore hypothesis (H_1) hold. Thus the proof is completed. □

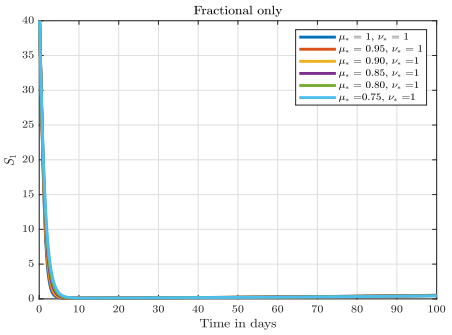

(a) Dynamics of Susceptible (S_1) Class

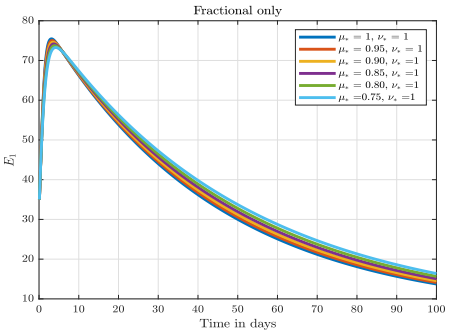

(b) Dynamics of Exposed (E_1) Class

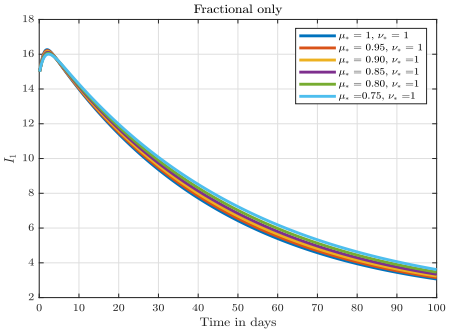

(c) Dynamics of Infected (I_1) class without Omicron variant

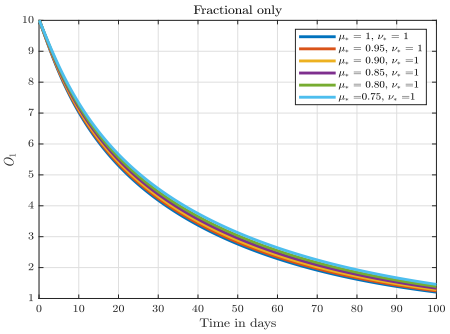

(d) Dynamics of Omicron variant Infected (O_1) class

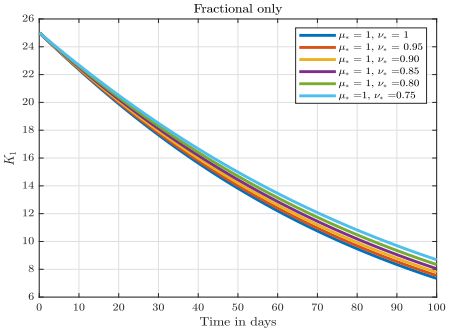

(e) Dynamics of Quarantine (K_1) Class

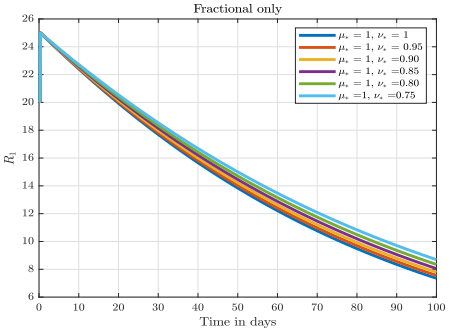

(f) Dynamics of Recovery (R_1) Class

Fig. 1. Numerical trajectory under different fractional order derivative, μ_*, and constant fractal dimension, ν_*, for Group-1.

Theorem 4.2. *Assume that* $\exists$ *a positive constant* $\Lambda > 0$ *such that*

$$\Lambda = \left(\frac{\nu_*(1-\mu_*)+\mu_*}{G(\mu_*)} \right) \mathbf{C}_* \leq 1, \tag{4.11}$$

then $\mathbf{A}_p$ *has a unique solution.*

Proof. Let $Y, \tilde{Y} \in \boldsymbol{Z}_*$, then we say

$$\begin{aligned} \|\mathbf{A}_p Y - \mathbf{A}_p \tilde{Y}\| &\leq \|\Omega_1^* Y - \Omega_1^* \tilde{Y}\| + \|\Omega_2^* Y - \Omega_2^* \tilde{Y}\|, \\ &\leq \frac{\nu_*(1-\mu_*)t^{\nu_*-1}}{G(\mu_*)} \Big| \max_{t\in[0,T]} |\Phi(t, Y(t)) - \Phi(t, \tilde{Y}(t))| \\ &+ \frac{\mu_*\nu_*}{G(\mu_*)} \max_{t\in[0,T]} \Big| \int_0^t \tau^{\nu_*-1} \Phi(\tau, Y(\tau)) d\tau \\ &- \int_0^t \tau^{\nu_*-1} \Phi(\tau, \tilde{Y}(\tau)) d\tau \Big|, \\ &\leq \left(\frac{\nu_*(1-\mu_*)+\mu_*}{G(\mu_*)} \right) \mathbf{C}_* \|Y - \tilde{Y}\|, \\ &= \Lambda \|Y - \tilde{Y}\|. \end{aligned} \tag{4.12}$$

Hence, hypothesis (H_2) hold, $\mathbf{A}_p$ has a unique fixed point. Consequently, two-age structure model for omicron SARS-CoV-2 variant has unique solution. □

5. Hyers-Ulam stability results

Definition 5.1. The two-age structure model for omicron SARS-CoV-2 variant is HU stable if for $\delta > 0$ and letting $Y \in \boldsymbol{Z}_*$ be any solution of below inequality

$$^{CFF}D_t^{\mu_*,\nu_*} Y(t) - \Psi(t, Y(t)) \leq \delta, \ \forall t \in [0, T]; \tag{5.1}$$

and with a unique solution $\tilde{Y}$ of problem (4.4) with a positive constant $\lambda_q > 0$, such that,

$$\|Y - \tilde{Y}\| \leq \lambda_q \delta, \ \forall t \in [0, T]. \tag{5.2}$$

Definition 5.2. Suppose that the function $\phi \in C(R, R)$, such that $\phi(0) = 0$ for any solution Y of (5.1) and $\tilde{Y}$ be unique solution of (4.4), then

$$\|Y - \tilde{Y}\| \leq \phi(\delta), \tag{5.3}$$

then the system (4.4) is generalized HU stable.

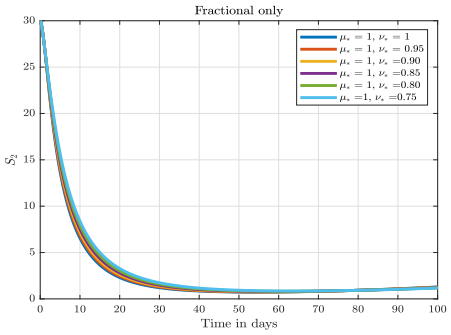

(a) Dynamics of Susceptible (S_2) Class

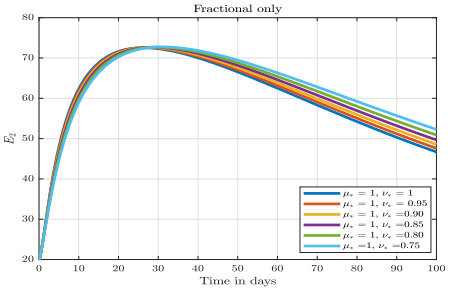

(b) Dynamics of Exposed (E_2) Class

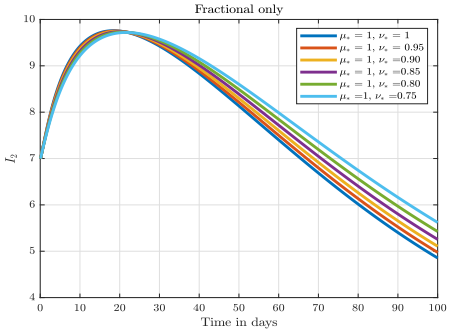

(c) Dynamics of Infected (I_2) class without Omicron variant

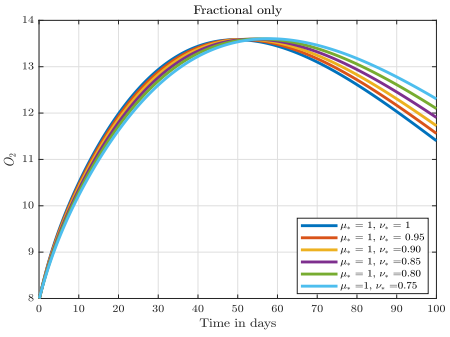

(d) Dynamics of Omicron variant Infected (O_2) class

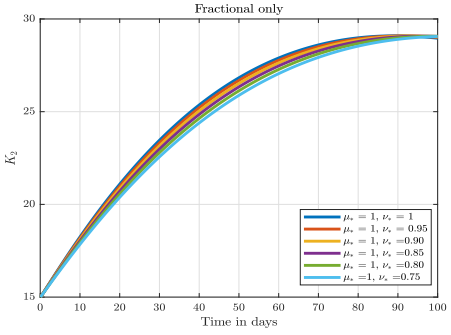

(e) Dynamics of Quarantine (K_2) Class

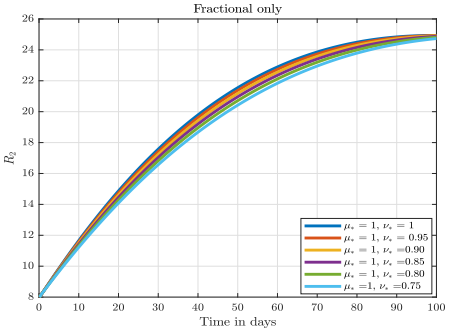

(f) Dynamics of Recovery (R_2) Class

Fig. 2. Numerical trajectory under different fractional order derivative, μ_*, and constant fractal dimension, ν_*, for Group-2.

Remark 5.3. Suppose $\chi(t) \in C([0,T],R)$, we say $Y \in \boldsymbol{Z}_*$ satisfies inequality (5.1) suppose that,

(i) $|\chi(t)| \leq \delta$, for all $t \in [0,T]$,

(ii) ${}^{CFF}D_t^{\mu_*}Y(t) = \Phi(t,Y(t)) + \chi(t)$, $\forall t \in [0,T]$.

We now take into account the system perturbation Eq. (4.4) as follows;

$$\begin{cases} {}^{CFF}D_t^{\mu_*,\nu_*}Y(t) = \Phi(t,Y(t)) + \chi(t), \\ Y(0) = Y_0. \end{cases} \tag{5.4}$$

The below Lemma is needed for our results.

Lemma 5.4. *From Eq. (5.4), we assume that the result of the following satisfy, thus,*

$$|Y(t) - \mathbf{A}_p\Phi(t,Y(t))| \leq [\frac{\nu_*(1-\mu_*)+\mu_*}{G(\mu_*)}]\delta.$$

Proof. *Let us consider Lemma 2.4, similarly, solution for Eq. (5.4) is given as;*

$$Y(t) = Y_0 + {}^{CFF}I_t^{\mu_*}\Phi(t,Y(t)) + {}^{CFF}I_t^{\mu_*}\chi(t).$$

Now, by (4.7), we deduce that

$$\begin{aligned} |Y(t) - \mathbf{A}_p\Phi(t,Y(t))| &\leq [\tfrac{\nu_*(1-\mu_*)t^{\nu_*-1}}{G(\mu_*)}|\chi(t)| + \tfrac{\mu_*\nu_*}{G(\mu_*)}\int_0^t \tau^{\nu_*-1}\Phi(\tau,Y(\tau))d\tau] \\ &\leq [\tfrac{\nu_*(1-\mu_*)+\mu_*}{G(\mu_*)}]\delta. \ \square \end{aligned} \tag{5.5}$$

Theorem 5.5. *Assume that the problem (4.4) is HU stable, such that*

$$\left(\frac{\nu_*(1-\mu_*)+\mu_*}{G(\mu_*)}\right)\mathbf{C}_* < 1.$$

Proof. *By Lemma 5.4, let $Y \in \boldsymbol{Z}_*$ be any solution and $\tilde{Y} \in \boldsymbol{Z}_*$ be unique solution for considered problem (4.4), then*

$$\begin{aligned} |Y(t) - \tilde{Y}(t)| &= |Y(t) - \mathbf{A}_p\tilde{Y}(t)| \\ &\leq |Y(t) - \mathbf{A}_pY(t)| + |\mathbf{A}_pY(t) - \mathbf{A}_p\tilde{Y}(t)| \\ &\leq [\tfrac{\nu_*(1-\mu_*)+\mu_*}{G(\mu_*)}]\delta + \left[\left(\tfrac{\nu_*(1-\mu_*)+\mu_*}{G(\mu_*)}\right)\mathbf{C}_*\right]\left\|Y - \tilde{Y}\right\| \\ &\leq \frac{[\frac{\nu_*(1-\mu_*)+\mu_*}{G(\mu_*)}]}{1-\left[\left(\frac{\nu_*(1-\mu_*)+\mu_*}{G(\mu_*)}\right)\mathbf{C}_*\right]}\delta. \end{aligned} \tag{5.6}$$

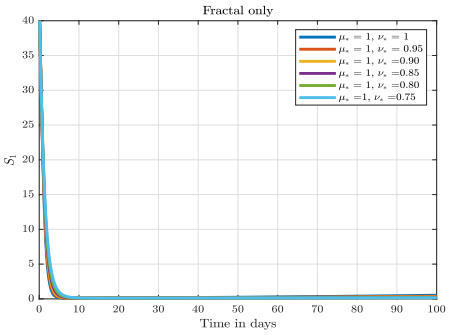

(a) Dynamics of Susceptible (S_1) Class

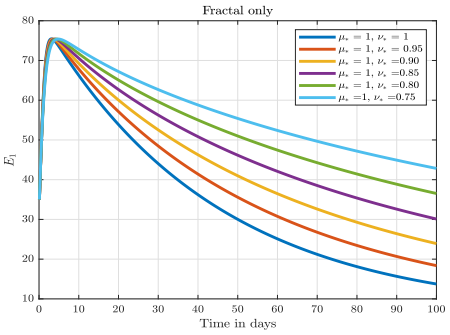

(b) Dynamics of Exposed (E_1) Class

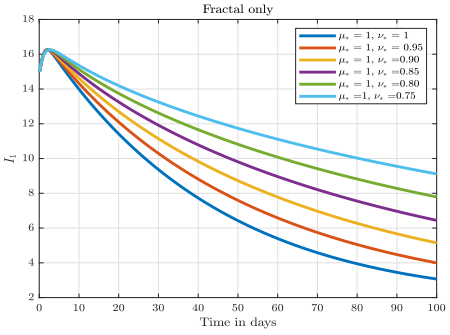

(c) Dynamics of Infected (I_1) class without Omicron variant

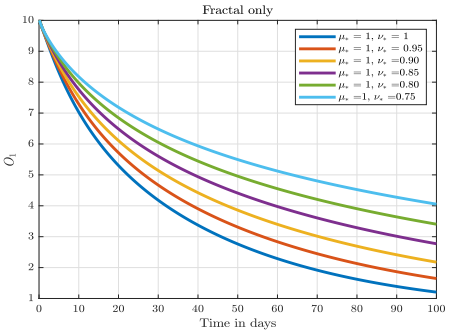

(d) Dynamics of Omicron variant Infected (O_1) class

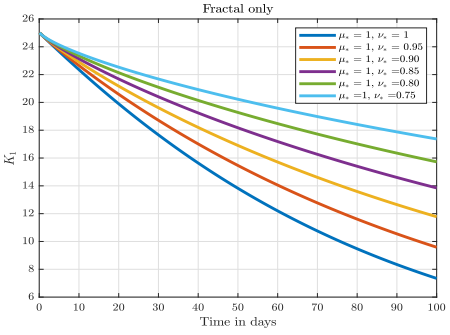

(e) Dynamics of Quarantine (K_1) Class

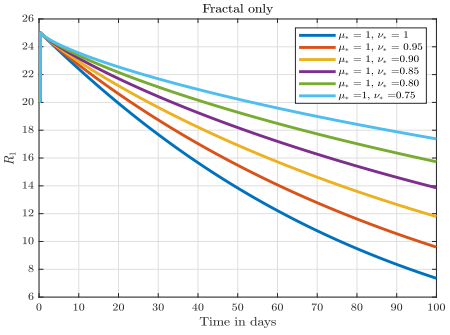

(f) Dynamics of Recovery (R_1) Class

Fig. 3. Numerical trajectory under different fractal dimension ν_*, and constant fractional order derivative, μ_*, for Group-1.

Thus,

$$\|Y(t)-\tilde{Y}(t)\| \leq \frac{[\frac{\nu_*(1-\mu_*)+\mu_*}{G(\mu_*)}]}{1-\Big[\big(\frac{\nu_*(1-\mu_*)+\mu_*}{G(\mu_*)}\big)\mathbf{C}_*\Big]}\delta.$$

Hence, we conclude that, the two-age structure model for omicron SARS-CoV-2 variant is HU stable. Consequently, it is generalized HU stable. □

6. Numerical scheme

The numerical methods for our suggested model, which is based on Newton polynomials, are provided in this section. For more details about Newton polynomials approximation see in Ref. 59. As presented in Ref. 59 in the case of the CFF-derivative, the Cauchy problem can be expressed as;

$$\begin{cases} {}^{CFF}D_t^{\mu_*\nu_*}Y(t)=\Phi(t,Y(t)), \\ Y(0)=Y_0. \end{cases} \tag{6.1}$$

The above (6.1) is equal to below equations

$$Y(t)=Y(0)+\frac{\nu_*(1-\mu_*)t^{\nu_*-1}}{G(\mu_*)}\Phi(t,Y(t))+\frac{\mu_*\nu_*}{G(\mu_*)}\int_0^t \tau^{\nu_*-1}\Phi(\tau,Y(\tau))d\tau. \tag{6.2}$$

At the point $t_{(n^*+1)}=(n^*+1)h$ and $t_{n^*}=n^*h$, $n^*=0,1,2,\ldots$, with h as time step. Let $F(t,Y(t))=\nu_* t^{\nu_*-1}\Phi(t,Y(t))$, then, we will get, when $t_{(n^*+1)}=(n^*+1)h$;

$$Y(t_{(n^*+1)})=Y(0)+\frac{(1-\mu_*)}{G(\mu_*)}F(t_{(z^*)},Y(t_{(n^*)}))+\frac{\mu_*}{G(\mu_*)}\int_0^{t_{n^*+1}} F(\tau,Y(\tau))d\tau, \tag{6.3}$$

and at the point $t_{n^*}=n^*h$

$$Y(t_{(n^*)})=Y(0)+\frac{(1-\mu_*)}{G(\mu_*)}F(t_{(n^*-1)},Y(t_{(n^*-1)}))+\frac{\mu_*}{G(\mu_*)}\int_0^{t_{n^*}} F(\tau,Y(\tau))d\tau. \tag{6.4}$$

Taking the difference of (6.3) and (6.4), we have

$$Y(t_{(n^*+1)}) = Y(t_{(n^*)}) + \frac{(1-\mu_*)}{G(\mu_*)}\left[\, F(t_{(n^*)}, Y(t_{(n^*)})) - F(t_{(n^*-1)}, Y(t_{(n^*-1)}))\,\right] + \frac{\mu_*}{G(\mu_*)}\int_0^{t_{n^*}} F(\tau, Y(\tau))d\tau. \tag{6.5}$$

To make things simpler, we may rewrite as

$$Y(t_{(n^*+1)}) = Y(t_{(n^*)}) + \frac{(1-\mu_*)}{G(\mu_*)}\left[\, F(t_{(n^*)}, Y(t_{(n^*)})) - F(t_{(n^*-1)}, Y(t_{(n^*-1)}))\,\right] \times \sum_{m^*=2}^{n^*}\int_{t_{m^*}}^{t_{m^*+1}} F(\tau, Y(\tau))d\tau. \tag{6.6}$$

Now, applying the Newton polynomial, (6.6) can be written as

$$\begin{aligned} Y^{n^*+1} &= Y^{n^*} + \frac{(1-\mu_*)}{G(\mu_*)}\left[\, F(t_{(n^*)}, Y(t_{(n^*)})) - F(t_{(n^*-1)}, Y(t_{(n^*-1)}))\,\right] \\ &+ \frac{\mu_*}{G(\mu_*)}\sum_{m^*=2}^{n^*}\left[\int_{t_{m^*}}^{t_{m^*+1}} \frac{F(t_{m^*-1}, Y^{m^*-1}) - F(t_{m^*-2}, Y^{m^*-2})}{h} \right. \\ &\times (\tau - t_{m^*-2})d\tau \\ &+ \int_{t_{m^*}}^{t_{m^*+1}} \frac{F(t_{m^*}, Y^{m^*}) - 2F(t_{m^*-1}, Y^{m^*-1}) + F(t_{m^*-2}, Y^{m^*-2})}{2h^2} \\ &\left.\times (s - t_{m^*-1})(\tau - t_{m^*-2})d\tau\right]. \end{aligned} \tag{6.7}$$

For further breakdown of (6.7) we get the following

$$\begin{aligned} Y^{n^*+1} &= Y^{n^*} + \frac{(1-\mu_*)}{G(\mu_*)}\left[\, F(t_{(n^*)}, Y(t_{(n^*)})) - F(t_{(n^*-1)}, Y(t_{(n^*-1)}))\,\right] \\ &+ \frac{\mu_*}{G(\mu_*)}\sum_{m^*=2}^{n^*}\left[\frac{F(t_{m^*-1}, Y^{m^*-1}) - F(t_{m^*-2}, Y^{m^*-2})}{h} \right. \\ &\times \int_{t_{m^*}}^{t_{m^*+1}} (\tau - t_{m^*-2})d\tau \\ &+ \int_{t_{m^*}}^{t_{m^*+1}} \frac{F(t_{m^*}, Y^{m^*}) - 2F(t_{m^*-1}, Y^{m^*-1}) + F(t_{m^*-2}, Y^{m^*-2})}{2h^2} \\ &\left.\times \int_{t_{m^*}}^{t_{m^*+1}} (\tau - t_{m^*-1})(\tau - t_{m^*-2})d\tau\right]. \end{aligned} \tag{6.8}$$

Now, solving integral equations in (6.8) by applying integration by substitution;

$$\begin{aligned} \int_{t_{m^*}}^{t_{m^*+1}} (\tau - t_{m^*-2})d\tau &= \frac{5}{2}h^2, \\ \int_{t_{m^*}}^{t_{m^*+1}} (\tau - t_{m^*-1})(\tau - t_{m^*-2})d\tau &= \frac{23}{6}h^3. \end{aligned} \tag{6.9}$$

Substituting Eq. (6.9) into (6.8), we have

$$\begin{aligned} Y^{n^*+1} &= Y^{n^*} + \frac{(1-\mu_*)}{G(\mu_*)}\left[\, F(t_{(n^*)}, Y(t_{(n^*)})) - F(t_{(n^*-1)}, Y(t_{(n^*-1)}))\,\right] \\ &+ \frac{\mu_*}{G(\mu_*)}\sum_{m^*=2}^{n^*}\left[\left(\, F(t_{m^*-1}, Y^{m^*-1}) - F(t_{m^*-2}, Y^{m^*-2})\,\right)(\frac{5}{2}h)\right. \\ &\left.+ \left(\, F(t_{m^*}, Y^{m^*}) - 2F(t_{m^*-1}, Y^{m^*-1}) + F(t_{m^*-2}, Y^{m^*-2})\,\right)(\frac{23}{12}h)\right]. \end{aligned} \tag{6.10}$$

For further breakdown of (6.10) we get the following scheme

$$\begin{aligned} Y^{n^*+1} &= Y^{n^*} + \frac{(1-\mu_*)}{G(\mu_*)}\left[\, F(t_{(n^*)}, Y(t_{(n^*)})) - F(t_{(n^*-1)}, Y(t_{(n^*-1)}))\,\right] \\ &+ \frac{\mu_*}{G(\mu_*)}\sum_{m^*=2}^{n^*}\left[\left(-\frac{4}{3}F(t_{m^*-1}, Y^{m^*-1})h\right.\right. \\ &\left.\left.+ \frac{5}{12}F(t_{m^*-2}, Y^{m^*-2})h + F(t_{r^*}, Y^{m^*})h\right)\right]. \end{aligned} \tag{6.11}$$

We substitute $\aleph(t, Y(t)) = \nu_* t^{\nu_*-1}\Phi(t, Y(t))$ into (6.11), then, we have the general Newton numerical scheme as follows;

$$\begin{aligned} Y^{n^*+1} &= Y^{n^*} + \frac{(1-\mu_*)}{G(\mu_*)}\left[\, \nu_* t_{n^*}^{\nu_*-1}\Phi(t_{(n^*)}, Y(t_{(n^*-1)})) \right. \\ &\left.- \nu_* t_{n^*-1}^{\nu_*-1}\Phi(t_{(n^*-1)}, Y(t_{(n^*-1)}))\,\right] \\ &+ \frac{\mu_*}{G(\mu_*)}\sum_{m^*=2}^{n^*}\left[\left(-\frac{4}{3}\nu_* t_{m^*-1}^{\nu_*-1}\Phi(t_{m^*-1}, Y^{m^*-1})h\right.\right. \\ &\left.\left.+ \frac{5}{12}\nu_* t_{m^*-2}^{\nu_*-1}\Phi(t_{m^*-2}, Y^{m^*-2})h + \frac{23}{12}\nu_* t_{m^*}^{\nu_*-1}\Phi(t_{m^*}, Y^{m^*})h\right)\right]. \end{aligned} \tag{6.12}$$

And for our two-age structure model for omicron SARS-CoV-2 variant (3.2) is given as follows;

$$\begin{aligned} S_1^{n^*+1} &= S_1^{n^*} + \frac{(1-\mu_*)}{G(\mu_*)}\left[\, \nu_* t_{n^*}^{\nu_*-1}Y_1(t_{n^*}, S_i^{n^*}, E_i^{n^*}, I_i^{n^*}, O_i^{n^*}, K_i^{n^*}, R_i^{n^*}) \right. \\ &\left.- \nu_* t_{n^*-1}^{\nu_*-1}Y_1(t_{n^*-1}, S_i^{n^*-1}, E_i^{n^*-1}, I_i^{n^*-1}, O_i^{n^*-1}, K_i^{n^*-1}, R_i^{n^*-1})\,\right] \\ &+ \frac{\mu_*}{G(\mu_*)}\sum_{m^*=2}^{n^*}\left[\left(-\frac{4}{3}\nu_* t_{m^*}^{\nu_*-1}Y_1(t_{m^*-1}, S_i^{m^*-1}, E_i^{m^*-1}, \right.\right. \\ &I_i^{m^*-1}, O_i^{m^*-1}, K_i^{m^*-1}, R_i^{m^*-1})h \\ &+ \frac{5}{12}\nu_* t_{m^*-2}^{\nu_*-1}Y_1(t_{m^*-2}, S_i^{m^*-2}, E_i^{m^*-2}, I_i^{m^*-2}, O_i^{m^*-2}, K_i^{m^*-2}, R_i^{m^*-2})h \\ &\left.\left.+ \frac{23}{12}\nu_* t_{m^*}^{\nu_*-1}Y_1(t_{m^*}, S_i^{m^*}, E_i^{m^*}, I_i^{m^*}, O_i^{m^*}, K_i^{m^*}, R_i^{m^*})h\right)\right]. \end{aligned} \tag{6.13}$$

$$\begin{aligned} E_1^{n^*+1} &= E_1^{n^*} + \frac{(1-\mu_*)}{G(\mu_*)}\left[\, \nu_* t_{n^*}^{\nu_*-1}Y_2(t_{n^*}, S_i^{n^*}, E_i^{n^*}, I_i^{n^*}, O_i^{n^*}, K_i^{n^*}, R_i^{n^*}) \right. \\ &\left.- \nu_* t_{n^*-1}^{\nu_*-1}Y_2(t_{n^*-1}, S_i^{n^*-1}, E_i^{n^*-1}, I_i^{n^*-1}, O_i^{n^*-1}, K_i^{n^*-1}, R_i^{n^*-1})\,\right] \\ &+ \frac{\mu_*}{G(\mu_*)}\sum_{m^*=2}^{n^*}\left[\left(-\frac{4}{3}\nu_* t_{m^*}^{\nu_*-1}Y_2(t_{m^*-1}, S_i^{m^*-1}, E_i^{m^*-1}, I_i^{m^*-1}, \right.\right. \\ &O_i^{m^*-1}, K_i^{m^*-1}, R_i^{m^*-1})h \\ &+ \frac{5}{12}\nu_* t_{m^*-2}^{\nu_*-1}Y_2(t_{m^*-2}, S_i^{m^*-2}, E_i^{m^*-2}, I_i^{m^*-2}, O_i^{m^*-2}, K_i^{m^*-2}, R_i^{m^*-2})h \\ &\left.\left.+ \frac{23}{12}\nu_* t_{m^*}^{\nu_*-1}Y_2(t_{m^*}, S_i^{m^*}, E_i^{m^*}, I_i^{m^*}, O_i^{m^*}, K_i^{m^*}, R_i^{m^*})h\right)\right]. \end{aligned} \tag{6.14}$$

$$\begin{aligned} I_1^{n^*+1} &= I_1^{n^*} + \frac{(1-\mu_*)}{G(\mu_*)}\left[\, \nu_* t_{n^*}^{\nu_*-1}Y_3(t_{n^*}, S_i^{n^*}, E_i^{n^*}, I_i^{n^*}, O_i^{n^*}, K_i^{n^*}, R_i^{n^*}) \right. \\ &\left.- \nu_* t_{n^*-1}^{\nu_*-1}Y_3(t_{n^*-1}, S_i^{n^*-1}, E_i^{n^*-1}, I_i^{n^*-1}, O_i^{n^*-1}, K_i^{n^*-1}, R_i^{n^*-1})\,\right] \\ &+ \frac{\mu_*}{G(\mu_*)}\sum_{m^*=2}^{n^*}\left[\left(-\frac{4}{3}\nu_* t_{m^*}^{\nu_*-1}Y_3(t_{m^*-1}, S_i^{m^*-1}, E_i^{m^*-1}, I_i^{m^*-1}, \right.\right. \\ &O_i^{m^*-1}, K_i^{m^*-1}, R_i^{m^*-1})h \\ &+ \frac{5}{12}\nu_* t_{m^*-2}^{\nu_*-1}Y_3(t_{m^*-2}, S_i^{m^*-2}, E_i^{m^*-2}, I_i^{m^*-2}, O_i^{m^*-2}, K_i^{m^*-2}, R_i^{m^*-2})h \\ &\left.\left.+ \frac{23}{12}\nu_* t_{m^*}^{\nu_*-1}Y_3(t_{m^*}, S_i^{m^*}, E_i^{m^*}, I_i^{m^*}, O_i^{m^*}, K_i^{m^*}, R_i^{m^*})h\right)\right]. \end{aligned} \tag{6.15}$$

$$\begin{aligned} O_1^{n^*+1} &= O_1^{n^*} + \frac{(1-\mu_*)}{G(\mu_*)}\left[\, \nu_* t_{n^*}^{\nu_*-1}Y_4(t_{n^*}, S_i^{n^*}, E_i^{n^*}, I_i^{n^*}, O_i^{n^*}, K_i^{n^*}, R_i^{n^*}) \right. \\ &\left.- \nu_* t_{n^*-1}^{\nu_*-1}Y_4(t_{n^*-1}, S_i^{n^*-1}, E_i^{n^*-1}, I_i^{n^*-1}, O_i^{n^*-1}, K_i^{n^*-1}, R_i^{n^*-1})\,\right] \\ &+ \frac{\mu_*}{G(\mu_*)}\sum_{m^*=2}^{n^*}\left[\left(-\frac{4}{3}\nu_* t_{m^*}^{\nu_*-1}Y_4(t_{m^*-1}, S_i^{m^*-1}, E_i^{m^*-1}, I_i^{m^*-1}, \right.\right. \\ &O_i^{m^*-1}, K_i^{m^*-1}, R_i^{m^*-1})h \\ &+ \frac{5}{12}\nu_* t_{m^*-2}^{\nu_*-1}Y_4(t_{m^*-2}, S_i^{m^*-2}, E_i^{m^*-2}, I_i^{m^*-2}, O_i^{m^*-2}, K_i^{m^*-2}, R_i^{m^*-2})h \\ &\left.\left.+ \frac{23}{12}\nu_* t_{m^*}^{\nu_*-1}Y_4(t_{m^*}, S_i^{m^*}, E_i^{m^*}, I_i^{m^*}, O_i^{m^*}, K_i^{m^*}, R_i^{m^*})h\right)\right]. \end{aligned} \tag{6.16}$$

$$K_1^{n^*+1} = K_1^{n^*} + \frac{(1-\mu_*)}{G(\mu_*)}\left[\nu_* t_{n^*}^{\nu_*-1} Y_5(t_{n^*}, S_i^{n^*}, E_i^{n^*}, I_i^{n^*}, O_i^{n^*}, K_i^{n^*}, R_i^{n^*}) - \nu_* t_{n^*-1}^{\nu_*-1} Y_5(t_{n^*-1}, S_i^{n^*-1}, E_i^{n^*-1}, I_i^{n^*-1}, O_i^{n^*-1}, K_i^{n^*-1}, R_i^{n^*-1})\right] + \frac{\mu_*}{G(\mu_*)}\sum_{m^*=2}^{n^*}\left[\left(-\frac{4}{3}\nu_* t_{m^*}^{\nu_*-1} Y_5(t_{m^*-1}, S_i^{m^*-1}, E_i^{m^*-1}, I_i^{m^*-1}, O_i^{m^*-1}, K_i^{m^*-1}, R_i^{m^*-1})h + \frac{5}{12}\nu_* t_{m^*-2}^{\nu_*-1} Y_5(t_{m^*-2}, S_i^{m^*-2}, E_i^{m^*-2}, I_i^{m^*-2}, O_i^{m^*-2}, K_i^{m^*-2}, R_i^{m^*-2})h + \frac{23}{12}\nu_* t_{m^*}^{\nu_*-1} Y_5(t_{m^*}, S_i^{m^*}, E_i^{m^*}, I_i^{m^*}, O_i^{m^*}, K_i^{m^*}, R_i^{m^*})h\right)\right]. \tag{6.17}$$

$$R_1^{n^*+1} = R_1^{n^*} + \frac{(1-\mu_*)}{G(\mu_*)}\left[\nu_* t_{n^*}^{\nu_*-1} Y_6(t_{n^*}, S_i^{n^*}, E_i^{n^*}, I_i^{n^*}, O_i^{n^*}, K_i^{n^*}, R_i^{n^*}) - \nu_* t_{n^*-1}^{\nu_*-1} Y_6(t_{n^*-1}, S_i^{n^*-1}, E_i^{n^*-1}, I_i^{n^*-1}, O_i^{n^*-1}, K_i^{n^*-1}, R_i^{n^*-1})\right] + \frac{\mu_*}{G(\mu_*)}\sum_{m^*=2}^{n^*}\left[\left(-\frac{4}{3}\nu_* t_{m^*}^{\nu_*-1} Y_6(t_{m^*-1}, S_i^{m^*-1}, E_i^{m^*-1}, I_i^{m^*-1}, O_i^{m^*-1}, K_i^{m^*-1}, R_i^{m^*-1})h + \frac{5}{12}\nu_* t_{m^*-2}^{\nu_*-1} Y_6(t_{m^*-2}, S_i^{m^*-2}, E_i^{m^*-2}, I_i^{m^*-2}, O_i^{m^*-2}, K_i^{m^*-2}, R_i^{m^*-2})h + \frac{23}{12}\nu_* t_{m^*}^{\nu_*-1} Y_6(t_{m^*}, S_i^{m^*}, E_i^{m^*}, I_i^{m^*}, O_i^{m^*}, K_i^{m^*}, R_i^{m^*})h\right)\right]. \tag{6.18}$$

$$S_2^{n^*+1} = S_2^{n^*} + \frac{(1-\mu_*)}{G(\mu_*)}\left[\nu_* t_{n^*}^{\nu_*-1} Y_7(t_{n^*}, S_i^{n^*}, E_i^{n^*}, I_i^{n^*}, O_i^{n^*}, K_i^{n^*}, R_i^{n^*}) - \nu_* t_{n^*-1}^{\nu_*-1} Y_7(t_{n^*-1}, S_i^{n^*-1}, E_i^{n^*-1}, I_i^{n^*-1}, O_i^{n^*-1}, K_i^{n^*-1}, R_i^{n^*-1})\right] + \frac{\mu_*}{G(\mu_*)}\sum_{m^*=2}^{n^*}\left[\left(-\frac{4}{3}\nu_* t_{m^*}^{\nu_*-1} Y_7(t_{m^*-1}, S_i^{m^*-1}, E_i^{m^*-1}, I_i^{m^*-1}, O_i^{m^*-1}, K_i^{m^*-1}, R_i^{m^*-1})h + \frac{5}{12}\nu_* t_{m^*-2}^{\nu_*-1} Y_7(t_{m^*-2}, S_i^{m^*-2}, E_i^{m^*-2}, I_i^{m^*-2}, O_i^{m^*-2}, K_i^{m^*-2}, R_i^{m^*-2})h + \frac{23}{12}\nu_* t_{m^*}^{\nu_*-1} Y_7(t_{m^*}, S_i^{m^*}, E_i^{m^*}, I_i^{m^*}, O_i^{m^*}, K_i^{m^*}, R_i^{m^*})h\right)\right]. \tag{6.19}$$

$$E_2^{n^*+1} = E_2^{n^*} + \frac{(1-\mu_*)}{G(\mu_*)}\left[\nu_* t_{n^*}^{\nu_*-1} Y_8(t_{n^*}, S_i^{n^*}, E_i^{n^*}, I_i^{n^*}, O_i^{n^*}, K_i^{n^*}, R_i^{n^*}) - \nu_* t_{n^*-1}^{\nu_*-1} Y_8(t_{n^*-1}, S_i^{n^*-1}, E_i^{n^*-1}, I_i^{n^*-1}, O_i^{n^*-1}, K_i^{n^*-1}, R_i^{n^*-1})\right] + \frac{\mu_*}{G(\mu_*)}\sum_{m^*=2}^{n^*}\left[\left(-\frac{4}{3}\nu_* t_{m^*}^{\nu_*-1} Y_8(t_{m^*-1}, S_i^{m^*-1}, E_i^{m^*-1}, I_i^{m^*-1}, O_i^{m^*-1}, K_i^{m^*-1}, R_i^{m^*-1})h + \frac{5}{12}\nu_* t_{m^*-2}^{\nu_*-1} Y_8(t_{m^*-2}, S_i^{m^*-2}, E_i^{m^*-2}, I_i^{m^*-2}, O_i^{m^*-2}, K_i^{m^*-2}, R_i^{m^*-2})h + \frac{23}{12}\nu_* t_{m^*}^{\nu_*-1} Y_8(t_{m^*}, S_i^{m^*}, E_i^{m^*}, I_i^{m^*}, O_i^{m^*}, K_i^{m^*}, R_i^{m^*})h\right)\right]. \tag{6.20}$$

$$I_2^{n^*+1} = I_2^{n^*} + \frac{(1-\mu_*)}{G(\mu_*)}\left[\nu_* t_{n^*}^{\nu_*-1} Y_9(t_{n^*}, S_i^{n^*}, E_i^{n^*}, I_i^{n^*}, O_i^{n^*}, K_i^{n^*}, R_i^{n^*}) - \nu_* t_{n^*-1}^{\nu_*-1} Y_9(t_{n^*-1}, S_i^{n^*-1}, E_i^{n^*-1}, I_i^{n^*-1}, O_i^{n^*-1}, K_i^{n^*-1}, R_i^{n^*-1})\right] + \frac{\mu_*}{G(\mu_*)}\sum_{m^*=2}^{n^*}\left[\left(-\frac{4}{3}\nu_* t_{m^*}^{\nu_*-1} Y_9(t_{m^*-1}, S_i^{m^*-1}, E_i^{m^*-1}, I_i^{m^*-1}, O_i^{m^*-1}, K_i^{m^*-1}, R_i^{m^*-1})h + \frac{5}{12}\nu_* t_{m^*-2}^{\nu_*-1} Y_9(t_{m^*-2}, S_i^{m^*-2}, E_i^{m^*-2}, I_i^{m^*-2}, O_i^{m^*-2}, K_i^{m^*-2}, R_i^{m^*-2})h + \frac{23}{12}\nu_* t_{m^*}^{\nu_*-1} Y_9(t_{m^*}, S_i^{m^*}, E_i^{m^*}, I_i^{m^*}, O_i^{m^*}, K_i^{m^*}, R_i^{m^*})h\right)\right]. \tag{6.21}$$

Table 2
Parameter values.

Parameter	Value	Parameter	Value	Assumed
Λ_1	0.099	Λ_2	0.015	Assumed
β_1	0.0207	β_2	0.0014	Assumed
β_3	0.00173	β_4	0.00120	Assumed
β_5	0.0001	β_6	0.001	Assumed
β_7	0.00313	β_8	0.00101	Assumed
β_9	0.0003	β_{10}	0.00101	Assumed
β_{11}	0.00117	β_{12}	0.000011	Assumed
μ_1	0.0001	μ_2	0.009	Assumed
γ_1	0.00015	γ_2	0.00023	Assumed
δ_1	0.0018	δ_2	0.00041	Assumed
ϵ_1	0.0021	ϵ_2	0.0021	Assumed
ϵ_3	0.0014	ϵ_4	0.0011	Assumed
α_1	0.000034	α_2	0.000037	Assumed
θ_1	0.00010	θ_2	0.00020	Assumed
σ_1	0.0080	σ_2	0.0051	Assumed
κ_1	0.0012	κ_2	0.0083	Assumed
ρ_1	0.0011	ρ_2	0.0017	Assumed
η_1	0.0041	η_2	0.003	Assumed
ϑ_1	0.09	ϑ_2	0.01	Assumed
ν_1	0.00002	ν_2	0.0003	Assumed
ω_1	0.002	ω_2	0.009	Assumed

$$O_2^{n^*+1} = O_2^{n^*} + \frac{(1-\mu_*)}{G(\mu_*)}\left[\nu_* t_{n^*}^{\nu_*-1} Y_{10}(t_{n^*}, S_i^{n^*}, E_i^{n^*}, I_i^{n^*}, O_i^{n^*}, K_i^{n^*}, R_i^{n^*}) - \nu_* t_{n^*-1}^{\nu_*-1} Y_{10}(t_{n^*-1}, S_i^{n^*-1}, E_i^{n^*-1}, I_i^{n^*-1}, O_i^{n^*-1}, K_i^{n^*-1}, R_i^{n^*-1})\right] + \frac{\mu_*}{G(\mu_*)}\sum_{m^*=2}^{n^*}\left[\left(-\frac{4}{3}\nu_* t_{m^*}^{\nu_*-1} Y_{10}(t_{m^*-1}, S_i^{m^*-1}, E_i^{m^*-1}, I_i^{m^*-1}, O_i^{m^*-1}, K_i^{m^*-1}, R_i^{m^*-1})h + \frac{5}{12}\nu_* t_{m^*-2}^{\nu_*-1} Y_{10}(t_{m^*-2}, S_i^{m^*-2}, E_i^{m^*-2}, I_i^{m^*-2}, O_i^{m^*-2}, K_i^{m^*-2}, R_i^{m^*-2})h + \frac{23}{12}\nu_* t_{m^*}^{\nu_*-1} Y_{10}(t_{m^*}, S_i^{m^*}, E_i^{m^*}, I_i^{m^*}, O_i^{m^*}, K_i^{m^*}, R_i^{m^*})h\right)\right]. \tag{6.22}$$

$$K_2^{n^*+1} = K_2^{n^*} + \frac{(1-\mu_*)}{G(\mu_*)}\left[\nu_* t_{n^*}^{\nu_*-1} Y_{11}(t_{n^*}, S_i^{n^*}, E_i^{n^*}, I_i^{n^*}, O_i^{n^*}, K_i^{n^*}, R_i^{n^*}) - \nu_* t_{n^*-1}^{\nu_*-1} Y_{11}(t_{n^*-1}, S_i^{n^*-1}, E_i^{n^*-1}, I_i^{n^*-1}, O_i^{n^*-1}, K_i^{n^*-1}, R_i^{n^*-1})\right] + \frac{\mu_*}{G(\mu_*)}\sum_{m^*=2}^{n^*}\left[\left(-\frac{4}{3}\nu_* t_{m^*}^{\nu_*-1} Y_{11}(t_{m^*-1}, S_i^{m^*-1}, E_i^{m^*-1}, I_i^{m^*-1}, O_i^{m^*-1}, K_i^{m^*-1}, R_i^{m^*-1})h + \frac{5}{12}\nu_* t_{m^*-2}^{\nu_*-1} Y_{11}(t_{m^*-2}, S_i^{m^*-2}, E_i^{m^*-2}, I_i^{m^*-2}, O_i^{m^*-2}, K_i^{m^*-2}, R_i^{m^*-2})h + \frac{23}{12}\nu_* t_{m^*}^{\nu_*-1} Y_{11}(t_{m^*}, S_i^{m^*}, E_i^{m^*}, I_i^{m^*}, O_i^{m^*}, K_i^{m^*}, R_i^{m^*})h\right)\right]. \tag{6.23}$$

$$R_2^{n^*+1} = R_2^{n^*} + \frac{(1-\mu_*)}{G(\mu_*)}\left[\nu_* t_{n^*}^{\nu_*-1} Y_{12}(t_{n^*}, S_i^{n^*}, E_i^{n^*}, I_i^{n^*}, O_i^{n^*}, K_i^{n^*}, R_i^{n^*}) - \nu_* t_{n^*-1}^{\nu_*-1} Y_{12}(t_{n^*-1}, S_i^{n^*-1}, E_i^{n^*-1}, I_i^{n^*-1}, O_i^{n^*-1}, K_i^{n^*-1}, R_i^{n^*-1})\right] + \frac{\mu_*}{G(\mu_*)}\sum_{m^*=2}^{n^*}\left[\left(-\frac{4}{3}\nu_* t_{m^*}^{\nu_*-1} Y_{12}(t_{m^*-1}, S_i^{m^*-1}, E_i^{m^*-1}, I_i^{m^*-1}, O_i^{m^*-1}, K_i^{m^*-1}, R_i^{m^*-1})h + \frac{5}{12}\nu_* t_{m^*-2}^{\nu_*-1} Y_{12}(t_{m^*-2}, S_i^{m^*-2}, E_i^{m^*-2}, I_i^{m^*-2}, O_i^{m^*-2}, K_i^{m^*-2}, R_i^{m^*-2})h + \frac{23}{12}\nu_* t_{m^*}^{\nu_*-1} Y_{12}(t_{m^*}, S_i^{m^*}, E_i^{m^*}, I_i^{m^*}, O_i^{m^*}, K_i^{m^*}, R_i^{m^*})h\right)\right]. \tag{6.24}$$

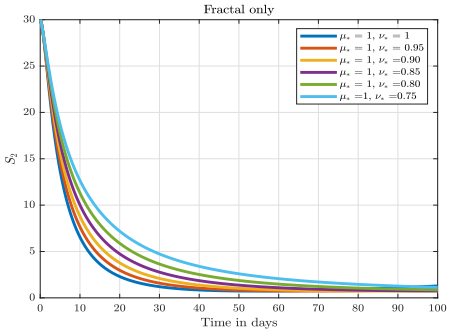

(a) Dynamics of Susceptible (S_2) Class

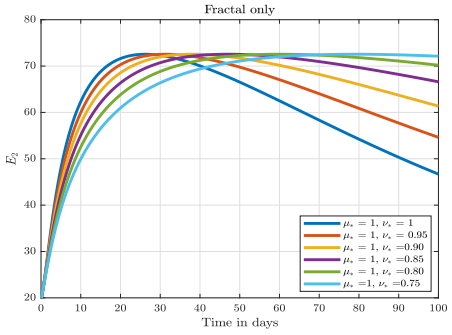

(b) Dynamics of Exposed (E_2) Class

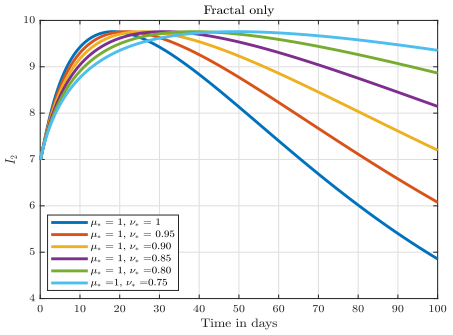

(c) Dynamics of Infected (I_2) class without Omicron variant

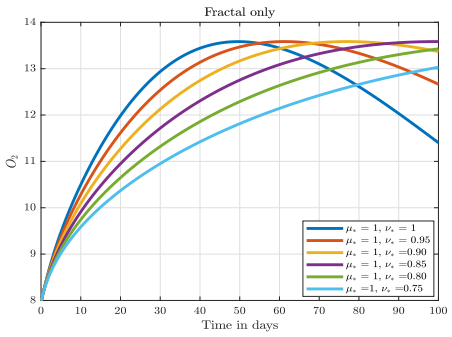

(d) Dynamics of Omicron variant Infected (O_2) class

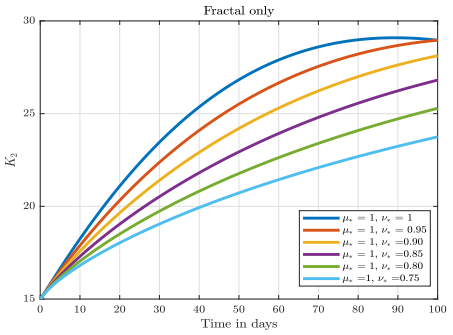

(e) Dynamics of Quarantine (K_2) Class

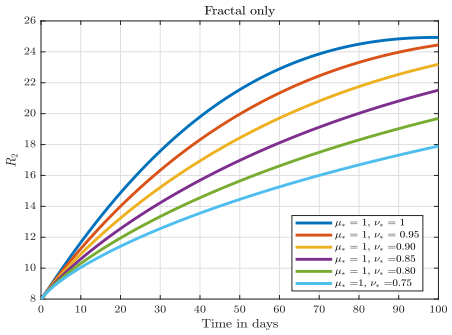

(f) Dynamics of Recovery (R_2) Class

Fig. 4. Numerical trajectory under different fractal dimension ν_*, and constant fractional order derivative, μ_*, for Group-2.

7. Numerical simulation and discussion

It is an old adage that a picture or image is worth a thousand words. In this section of our paper, we use the suggested numerical scheme to present numerical simulations for the fractal–fractional two-age structure model for omicron SARS-CoV-2 variant. To achieve this, we take account the following initial conditions; $S_1(0) = 40$; $E_1(0) = 35$; $I_1(0) = 15$; $O_1(0) = 10$; $K_1(0) = 25$; $R_1(0) = 20$; $S_2(0) = 30$; $E_2(0) = 20$; $I_2(0) = 7$; $O_2(0) = 8$; $K_2(0) = 15$; $R_2(0) = 8$, with assumed parameter values in Table 2. For the fractal–fractional two-age structure model for omicron SARS-CoV-2 variant, the numerical trajectory are shown in Figs. 1–6. In Fig. 1(a)–(e), we kept the fractal dimension constant $\nu_* = 1$ and changed fractional order μ_*, we observed that in Fig. 1(a) there is convergency between the fractional order μ_* and the integer order at the end of the simulation time. We also observed that in Fig. 1(a)–(f) there is proportionality between fractional order derivative μ_* and the rate of individuals joining each compartment. This means that when we increase the fractional value the individual population increases, which then means that using fractional order we can obtain clear qualitative information on omicron SARS-CoV-2 variant. In Fig. 2, although the trajectory is similar to Fig. 1, but the different is that, in Fig. 2(f) when we increase the fractional value, we capture more recovery population as to in Fig. 1(f). From Fig. 3 and Fig. 4, when we maintained the fractional order derivative as constant $\mu_* = 1$ and

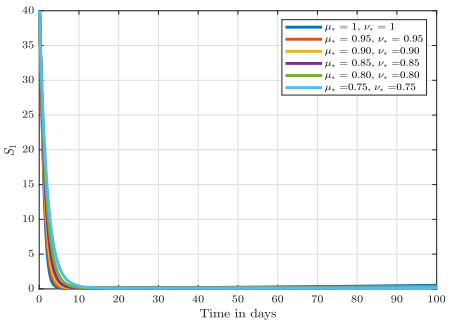

(a) Dynamics of Susceptible (S_1) Class

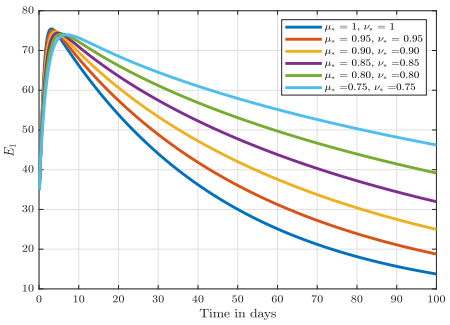

(b) Dynamics of Exposed (E_1) Class

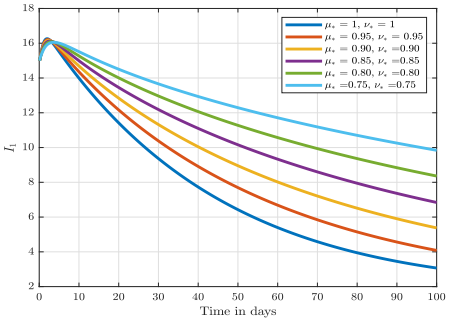

(c) Dynamics of Infected (I_1) class without Omicron variant

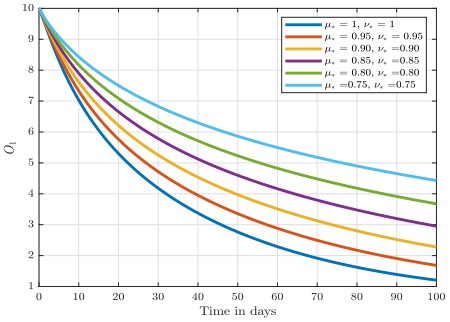

(d) Dynamics of Omicron variant Infected (O_1) class

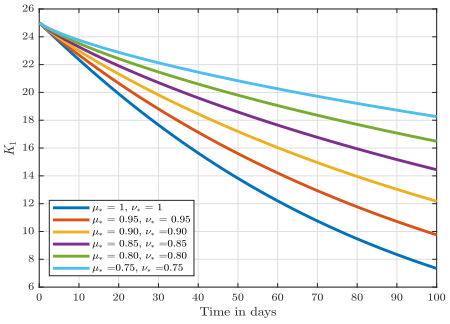

(e) Dynamics of Quarantine (K_1) Class

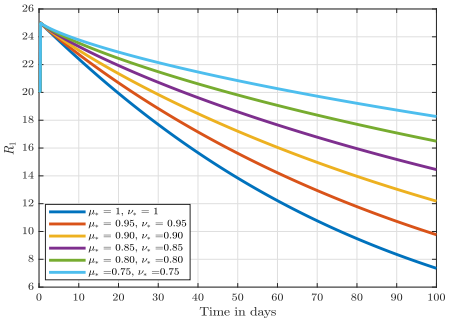

(f) Dynamics of Recovery (R_1) Class

Fig. 5. Numerical trajectory under different fractal dimension ν_*, and different fractional order derivative, μ_*, for Group-1.

changed fractal dimension ν_*, we observed that all the subplots in Figs. 3 and 4 have proportionality between fractal dimension ν_* and the rate of individuals joining each compartment or subplots. This indicates that fractal dimension has significant influences on the control of omicron SARS-CoV-2 variant. In Figs. 5 and 6, when the fractional order μ_* and fractal dimension ν_* are simultaneously reduced from 1, the rate of recovery increases significantly, and there is a distinct behaviours in recovery compartment in both Group-1 and Group-2. This indicates that combining fractal–fractional operators directly affect the dynamics of the two-age structure and shows hidden behaviours of omicron SARS-CoV-2 variant among the two age.

8. Conclusion

In this paper, a new mathematical model for two-age structure omicron SARS-CoV-2 variant transmission dynamism has been investigated using Caputo–Fabrizio fractal–fractional technique. The important mathematical assessments including the existence and uniqueness of the epidemic model have been proved using the fixed point theorem of Banach and Krasnoselskii's type. The stability of the proposed model have been proved under HU stability-type. The modified Newton polynomial was utilized to obtained the iterative solution for our proposed model. Simulation has been made to demonstrate the impact of the

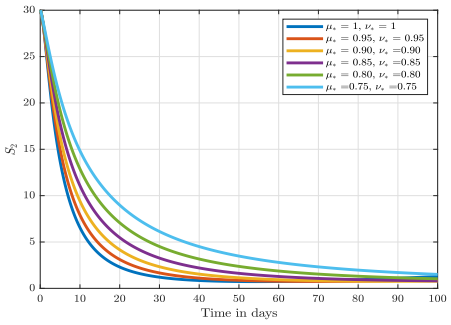

(a) Dynamics of Susceptible (S_2) Class

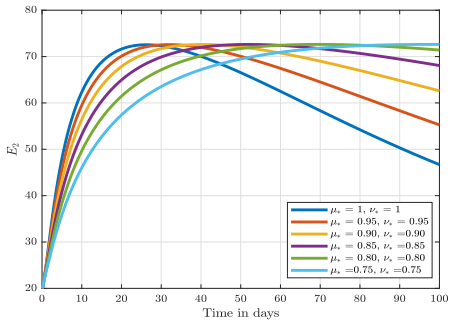

(b) Dynamics of Exposed (E_2) Class

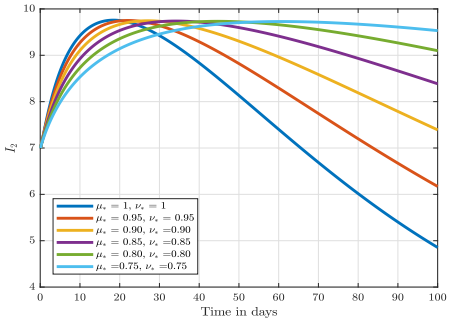

(c) Dynamics of Infected (I_2) class without Omicron variant

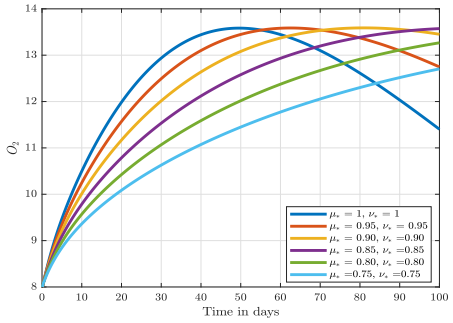

(d) Dynamics of Omicron variant Infected (O_2) class

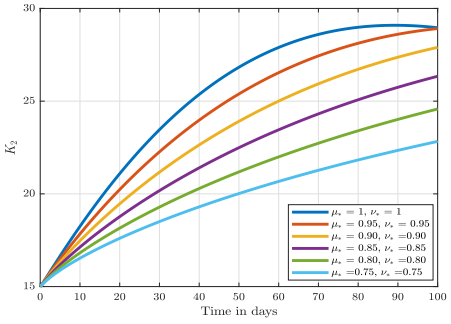

(e) Dynamics of Quarantine (K_2) Class

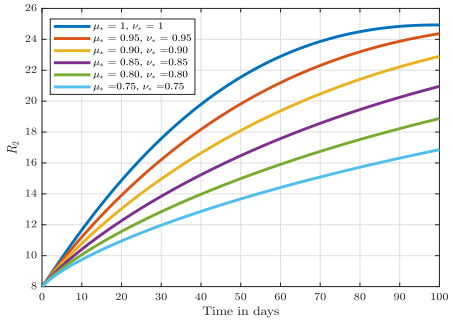

(f) Dynamics of Recovery (R_2) Class

Fig. 6. Numerical trajectory under different fractal dimension ν_*, and different fractional order derivative, μ_*, for Group-2.

fractional and fractal orders for the analysis of the omicron SARS-CoV-2 variant dynamics among the two-age groups in a community. One can observe from the graphical results that reducing the fractal–fractional order, the infection and recovery increase in Group-1. While reducing the fractal–fractional order, the infection increase but recovery decrease in Group-2. The combined operators provide very effective results for the proposed model as compared to the single order case. Due to such results, we aim to design other mathematical model involving optimal control parameters in the next papers.

CRediT authorship contribution statement

Emmanuel Addai: Conceptualization, Methodology, Formal analysis, Software, Visualization, Writing – original draft, Writing – review & editing. **Lingling Zhang:** Supervision, Methodology, Formal analysis, Software, Visualization, Writing – review & editing. **Joshua Kiddy K. Asamoah:** Supervision, Methodology, Formal analysis, Software, Visualization, Writing – review & editing. **Ama Kyerewaa Preko:** Formal analysis, Writing – review & editing. **Yarhands Dissou Arthur:** Formal analysis, Writing – review & editing.

Declaration of competing interest

The authors declare that they have no known competing financial interests or personal relationships that could have appeared to influence the work reported in this paper.

Data availability

No data was used for the research described in the article.

Acknowledgment

The First and Second author acknowledge the support of Key R&D program of Shanxi Province, China (International Cooperation, 201903D421042) and Research Project Supported by Shanxi Scholarship Council of China (2021-030).

References

1. WHO. Coronavirus disease (COVID-19), What are the symptoms of COVID-19?https://www.who.int/emergencies/diseases/novel-coronavirus-2019/question-and-answers-hub/q-a-detail/coronavirus-disease-covid-19.

2. Asamoah JKK, Owusu MA, Jin Z, et al. Global stability and cost-effectiveness analysis of COVID-19 considering the impact of the environment: using data from Ghana. *Chaos Solitons Fractals*. 2020;140:110103.
3. Asamoah JKK, Jin Z, Sun GQ, Seidu B, Yankson E, Abidemi A, Oduro FT, Moore SE, Okyere E. Sensitivity assessment and optimal economic evaluation of a new COVID-19 compartmental epidemic model with control interventions. *Chaos Solitons Fractals*. 2021;146:110885.
4. Sigdel A, Bista A, Bhattarai N, Pun BC, Giri G, Marqusee H, Thapa S. Depression, anxiety and depression-anxiety comorbidity amid COVID-19 pandemic: An online survey conducted during lockdown in Nepal. 2020 MedRxiv.
5. Ahmed MZ, Ahmed O, Aibao Z, et al. Epidemic of COVID-19 in China and associated psychological problems. *Asian J Psychiatry*. 2020;51:102092.
6. Meda N, Pardini S, Slongo I, Bodini L, Rigobello P, Visioli F, Novara C. COVID-19 and depressive symptoms in students before and during lockdown. 2020 MedRxiv.
7. Djernes JK. Prevalence and predictors of depression in populations of elderly: a review. *Acta Psychiatr Scand*. 2006;113(5):372–387.
8. Li D, Zhang DJ, Shao JJ, Qi XD, Tian L. A meta-analysis of the prevalence of depressive symptoms in Chinese older adults. *Arch Gerontol Geriat*. 2014;58(1):1–9.
9. Pulliam JR, van Schalkwyk C, Govender N, von Gottberg A, Cohen C, Groome MJ, Dushoff J, Mlisana K, Moultrie H. Increased risk of SARS-CoV-2 reinfection associated with emergence of Omicron in South Africa. *Science*. 2022;376(6593):eabn4947.
10. Miller NL, Clark T, Raman R, Sasisekharan R. Insights on the mutational landscape of the SARS-CoV-2 Omicron variant. 2021 BioRxiv.
11. Liu Y, Liu J, Johnson BA, Xia H, Ku Z, Schindewolf C, Widen SG, An Z, Weaver SC, Menachery VD, Xie X. Delta spike P681R mutation enhances SARS-CoV-2 fitness over Alpha variant. 2021. bioRxiv. preprint, 10(2021.08), 12–456173. 2021.
12. Liu Y, Liu J, Plante KS, Plante JA, Xie X, Zhang X, Ku Z, An Z, Scharton D, Schindewolf C, Menachery VD. The N501Y spike substitution enhances SARS-CoV-2 transmission. 2021 BioRxiv.
13. Ku Z, Xie X, Davidson E, Ye X, Su H, Menachery VD, Li Y, Yuan Z, Zhang X, Muruato AE, Tyrell B. Author correction: Molecular determinants and mechanism for antibody cocktail preventing SARS-CoV-2 escape. *Nature Commun*. 2021;12(1):1.
14. Zhou D, Dejnirattisai W, Supasa P, Liu C, Mentzer AJ, Ginn HM, Zhao Y, Duyvesteyn HM, Tuekprakhon A, Nutalai R, Wang B. Evidence of escape of SARS-CoV-2 variant B, 1.351 from natural and vaccine-induced Sera. *Cell*. 2021;184(9):2348–2361.
15. Yu Y, Liu Y, Zhao S, He D. A simple model to estimate the transmissibility of SARS-CoV-2 Beta, Delta and Omicron variants in South Africa. Delta and omicron variants in South Africa, Available at SSRN (December 20, 2021). 2021.
16. Yang W, Shaman J. COVID-19 pandemic dynamics in South Africa and epidemiological characteristics of three variants of concern (Beta, Delta, and Omicron). 2022 medRxiv: the preprint server for health sciences, 2021–12.
17. Lyngse FP, Kirkeby CT, Denwood M, Christiansen LE, Mølbak K, Møller CH, Skov RL, Krause TG, Rasmussen M, Sieber RN, Johannesen TB. Transmission of SARS-CoV-2 Omicron VOC subvariants BA. 1 and BA. 2: evidence from Danish households. 2022 MedRxiv.
18. Tegally H, Moir M, Everatt J, Giovanetti M, Scheepers C, Wilkinson E, Subramoney K, Makatini Z, Moyo S, Amoako DG, Baxter C. Emergence of SARS-CoV-2 omicron lineages BA, 4 and BA. 5 in South Africa. *Nat Med*. 2022:1–6.
19. McMahan K, Giffin V, Tostanoski LH, Chung B, Siamatu M, Suthar MS, Halfmann P, Kawaoka Y, Piedra-Mora C, Jain N, Ducat S. Reduced pathogenicity of the SARS-CoV-2 Omicron variant in hamsters. *Med*. 2022;3(4):262–268.
20. Suzuki R, Yamasoba D, Kimura I, Wang L, Kishimoto M, Ito J, Morioka Y, Nao N, Nasser H, Uriu K, Kosugi Y. Attenuated fusogenicity and pathogenicity of SARS-CoV-2 Omicron variant. *Nature*. 2022;603(7902):700–705.
21. Miller NL, Clark T, Raman R, Sasisekharan R. Insights on the mutational landscape of the SARS-CoV-2 Omicron variant receptor-binding domain. *Cell Rep Med*. 2022;3(2):100527.
22. Hussein T, Hammad MH, Surakhi O, AlKhanafseh M, Fung PL, Zaidan MA, Wraith D, Ershaidat N. Short-term and long-term COVID-19 pandemic forecasting revisited with the emergence of OMICRON variant in Jordan. *Vaccines*. 2022;10(4):569.
23. Tong C, Shi W, Zhang A, Shi Z. Tracking and controlling the spatiotemporal spread of SARS-CoV-2 Omicron variant in South Africa. *Travel Med Infect Dis*. 2022;46:102252.
24. Ko Y, Mendoza VM, Mendoza R, Seo Y, Lee J, Lee J, Kwon D, Jung E. Multifaceted analysis of COVID-19 epidemic in Korea considering omicron variant: mathematical modeling-based study. *J Korean Med Sci*. 2022;37(26).
25. Eales O, Martins LdeOliveira, Page AJ, Wang H, Bodinier B, Tang D, Haw D, Jonnerby J, Atchison C, Ashby D, Barclay W. Dynamics of competing SARS-CoV-2 variants during the Omicron epidemic in England. *Nature Commun*. 2022;13(1):1–11.
26. Wang J, Chan YC, Niu R, Wong EW, van Wyk MA. Modeling the impact of vaccination on COVID-19 and Its Delta and Omicron variants. *Viruses*. 2022;14(7):1482.
27. Ssebuliba J, Nakakawa JN, Ssematimba A, Mugisha JYT. Mathematical modelling of COVID-19 transmission dynamics in a partially comorbid community. *Partial Differ Equ Appl Math*. 2022;5:100212.
28. Acheampong E, Okyere E, Iddi S, Bonney JH, Asamoah JKK, Wattis JA, Gomes RL. Mathematical modelling of earlier stages of COVID-19 transmission dynamics in Ghana. *Results Phys*. 2022;34:105193.
29. Faniran TS, Ali A, Al-Hazmi NE, et al. New variant of SARS-CoV-2 dynamics with imperfect vaccine. *Complexity*. 2022;2022.
30. Asamoah JKK, Bornaa CS, Seidu B, Jin Z. Mathematical analysis of the effects of controls on transmission dynamics of SARS-CoV-2. *Alex Eng J*. 2020;59(6):5069–5078.
31. Asamoah JKK, Okyere E, Abidemi A, Moore SE, Sun GQ, Jin Z, Acheampong E, Gordon JF. Optimal control and comprehensive cost-effectiveness analysis for COVID-19. *Results Phys*. 2022;33:105177.
32. Asamoah JKK, Okyere E, Yankson E, Opoku AA, Adom-Konadu A, Acheampong E, Arthur YD. Non-fractional and fractional mathematical analysis and simulations for Q fever. *Chaos Solitons Fractals*. 2022;156:111821.
33. Omame A, Abbas M, Onyenegecha CP. A fractional-order model for COVID-19 and tuberculosis co-infection using Atangana–Baleanu derivative. *Chaos Solitons Fractals*. 2021;153:111486.
34. Omame A, Okuonghae D, Nwajeri UK, Onyenegecha CP. A fractional-order multi-vaccination model for COVID-19 with non-singular kernel. *Alex Eng J*. 2022;61(8):6089–6104.
35. Omame A, Abbas M, Onyenegecha CP. A fractional order model for the co-interaction of COVID-19 and Hepatitis B virus. *Results Phys*. 2022;37:105498.
36. Kumar S, Kumar A, Samet B, Gómez-Aguilar JF, Osman MS. A chaos study of tumor and effector cells in fractional tumor-immune model for cancer treatment. *Chaos Solitons Fractals*. 2020;141:110321.
37. Kumar S, Chauhan RP, Momani S, Hadid S. Numerical investigations on COVID-19 model through singular and non-singular fractional operators. *Numer Methods Partial Differ Equ*. 2020.
38. Mohammadi H, Kumar S, Rezapour S, Etemad S. A theoretical study of the Caputo–Fabrizio fractional modeling for hearing loss due to Mumps virus with optimal control. *Chaos Solitons Fractals*. 2021;144:110668.
39. Kumar S, Kumar R, Osman MS, Samet B. A wavelet based numerical scheme for fractional order SEIR epidemic of measles by using Genocchi polynomials. *Numer Methods Partial Differential Equations*. 2021;37(2):1250–1268.
40. Kumar S, Ahmadian A, Kumar R, Kumar D, Singh J, Baleanu D, Salimi M. An efficient numerical method for fractional SIR epidemic model of infectious disease by using Bernstein wavelets. *Mathematics*. 2020;8(4):558.
41. Addai E, Zhang L, Preko AK, Asamoah JK. Fractional order epidemiological model of SARS-CoV-2 dynamism involving Alzheimer's disease. *Healthc Anal*. 2022:100114.
42. Zhang L, Addai E, Ackora-Prah J, Arthur YD, Asamoah JKK. Fractional-order Ebola-Malaria coinfection model with a focus on detection and treatment rate. *Comput Math Methods Med*. 2022.
43. Atangana A, İğret Araz S. Mathematical model of COVID-19 spread in Turkey and South Africa: theory, methods, and applications. *Adv Differ Equ*. 2020;2020(1):1–89.
44. Atangana A. Fractal-fractional differentiation and integration: connecting fractal calculus and fractional calculus to predict complex system. *Chaos Solitons Fractals*. 2017;102:396–406.
45. Li YM, Ullah S, Khan MA, Alshahrani MY, Muhammad T. Modeling and analysis of the dynamics of HIV/AIDS with non-singular fractional and fractal-fractional operators. *Phys Scr*. 2021;96(11):114008.
46. Asamoah JKK. Fractal-fractional model and numerical scheme based on Newton polynomial for Q fever disease under Atangana–Baleanu derivative. *Results Phys*. 2022;34:105189.
47. Addai E, Zhang L, Ackora-Prah J, et al. Fractal-fractional order dynamics and numerical simulations of a Zika epidemic model with insecticide-treated nets. *Physica A*. 2022;603:127809.
48. Rezapour S, Asamoah JKK, Hussain A, Ahmad H, Banerjee R, Etemad S, Botmart T. A theoretical and numerical analysis of a fractal-fractional two-strain model of meningitis. *Results Phys*. 2022;39:105775.
49. Arik İA, Araz Sİ. Crossover behaviors via piecewise concept: A model of tumor growth and its response to radiotherapy. *Results Phys*. 2022;41:105894.
50. Okyere E, Seidu B, Nantomah K, Asamoah JKK. Fractal-fractional SIRS epidemic model with temporary immunity using Atangana-Baleanu derivative. *Commun Math Biol Neurosci*. 2022;2022.
51. Paul S, Mahata A, Mukherjee S, Roy B. Dynamics of SIQR epidemic model with fractional order derivative. *Partial Differ Equ Appl Math*. 2022;5:100216.
52. Mahata A, Paul S, Mukherjee S, Roy B. Stability analysis and hopf bifurcation in fractional order SEIRV epidemic model with a time delay in infected individuals. *Partial Differ Equ Appl Math*. 2022;5:100282.
53. Li T, Guo Y. Optimal control and cost-effectiveness analysis of a new COVID-19 model for Omicron strain. *Physica A*. 2022;606:128134.
54. Xu C, Farman M, Hasan A, Akgül A, Zakarya M, Albalawi W, Park C. Lyapunov stability and wave analysis of Covid-19 omicron variant of real data with fractional operator. *Alex Eng J*. 2022.
55. Wang BG, Wang ZC, Wu Y, et al. A mathematical model reveals the influence of NPIs and vaccination on SARS-CoV-2 Omicron variant. *Res Square*. 2022.

56. Cai M, Em Karniadakis G, Li C. Fractional SEIR model and data-driven predictions of COVID-19 dynamics of Omicron variant. *Chaos*. 2022;32(7):071101.
57. Farman M, Amin M, Akgül A, et al. Fractal fractional operator for COVID-19 (Omicron) variant outbreak with analysis and modeling. *Results Phys*. 2022:105630.
58. Sher M, Shah K, Khan ZA, Khan H, Khan A. Computational and theoretical modeling of the transmission dynamics of novel COVID-19 under Mittag-Leffler power law. *Alex Eng J*. 2020;59(5):3133–3147.
59. Atangana A, Araz SI. *New Numerical Scheme with Newton Polynomial: Theory, Methods, and Applications*. Academic Press, Elsevier; 2021.